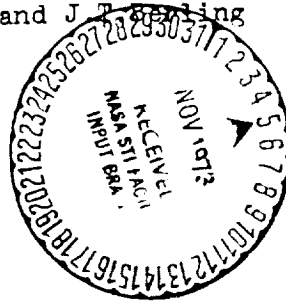NASA CR-121260

# HIGH TEMPERATURE, LOW-CYCLE FATIGUE

## OF COPPER-BASE ALLOYS IN ARGON;

## PART II - ZIRCONIUM-COPPER AT 482,

## 538 AND 593°C.

by:  J.B.Conway,R.H.Stentz and J.T.Berling

## MAR-TEST INC.

Cincinnati,Ohio

August,1973

prepared for

# NATIONAL AERONAUTICS AND SPACE ADMINISTRATION

# TABLE OF CONTENTS

page

# I - SUMMARY

This report describes the test results obtained in the Task 2 portion of this contract which involved a fairly detailed study of the short-term tensile and low-cycle fatigue behavior of zirconium-copper (1/2 hard) in argon at elevated temperatures. A total of 35 tests was performed in determinations of the temperature and strain rate effects on tensile properties, the modulus of elasticity from room temperature to 593°C, the temperature effect on the low-cycle fatigue life at a strain rate of $2 \times 10^{-3}$ sec$^{-1}$, and the effect of strain rate and hold time on the low-cycle fatigue life at 538°C. Hourglass-shaped specimens were used in conjunction with a diametral extensometer in the evaluations of the short-term tensile and low-cycle fatigue properties while a cylindrical gage section specimen was used in conjunction with an axial extensometer in the modulus of elasticity measurements which were made in air.

These studies showed that the modulus of elasticity of the zirconium-copper alloy decreased from 115,000 to 70,000 MN/m$^2$ as the temperature increased from room temperature to 593°C. It was also shown that the 0.2% yield and ultimate tensile strength of the zirconium-copper alloy decreased with increasing temperature reaching values close to 150 MN/m$^2$ at 593°C. Reduction in area increased slightly with increasing temperature and reached a value close to 90 percent at 593°C. In the axial-strain-controlled low-cycle fatigue tests it was found that the fatigue resistance at 482°C was essentially identical to that observed at 593°C and that this behavior was essentially identical to that observed at 538°C in the Task 1 effort. Decreased strain rates and hold periods in tension reduced the fatigue life at 538°C while hold times in compression had no effect on the fatigue life at this temperature. Stress relaxation curves obtained in the hold-time tests indicate very similar results for the tension and compression relaxations although in the first second or so the tension relaxation appeared to be more rapid. After the first cycle or so the ratio of the amount of relaxation per cycle divided by the stress at the start of the cycle remained constant for essentially the entire test.

## II - INTRODUCTION

Regeneratively-cooled, reusable-rocket nozzle liners such as found in the engines of the Space Shuttle, Orbit-to-Orbit Shuttle, Space Tug, etc., undergo a severe thermal strain cycle during each firing. To withstand the severe cycles, the liner material must have a proper combination of high thermal conductivity and high low-cycle fatigue resistance. Copper-base alloys possess these desirable qualities and were thusly chosen for this program. The purpose of the investigation is to screen a variety of candidate alloys, select the most promising for the application, and to generate material property data that are required in the design and life prediction of rocket nozzle liners.

In the Task 1 effort (see NASA CR 121259) on this program a detailed screening evaluation was performed to provide an assessment of the tensile and fatigue properties of 12 candidate materials (11 copper-base alloys and silver) at temperatures to $538^{\circ}C$. Short-term tensile tests were performed in duplicate using a strain rate of $2 \times 10^{-3}$ $sec^{-1}$ to provide measurements of the 0.2% yield strength, ultimate tensile strength and reduction in area at room temperature and at $538^{\circ}C$. Low-cycle fatigue evaluations were performed at $538^{\circ}C$ using an axial strain rate of $2 \times 10^{-3}$ $sec^{-1}$ in completely reversed (A-ratio of infinity), axial strain controlled tests based on axial loading. All room temperature evaluations were performed in air while all tests at $538^{\circ}C$ were performed in high purity argon in which the oxygen level was maintained below 0.01 percent by volume. Hourglass-shaped specimens and diametral extensometry were employed in both the tensile and fatigue evaluations while the use of an analog strain computer enabled the fatigue tests to be performed in axial strain control.

After the Task 1 effort was completed the NASA Project Manager performed a detailed review of all the material property information pertaining to the 12 candidate materials and selected one material to be tested in additional detail in the Task 2 portion of this program. This material was the R-2 alloy, zirconium-copper, 1/2 Hard.

The material property measurements specified for the Task 2 effort included the following:
1) short-term tensile at $482^{\circ}$ and $593^{\circ}C$ using a strain rate of $2 \times 10^{-3}$ $sec^{-1}$;
2) short-term tensile at $538^{\circ}C$ using strain rates of

$4 \times 10^{-4}$ and $1 \times 10^{-2}$ sec$^{-1}$;

3) modulus of elasticity from room temperature to 593°C using a strain rate of $2 \times 10^{-3}$ sec $^{-1}$;

4) strain-controlled low-cycle fatigue behavior at 482° and 593°;

5) strain-controlled low-cycle fatigue behavior at 538°C using strain rates of $4 \times 10^{-4}$ and $1 \times 10^{-2}$ sec$^{-1}$;

and 6) strain-controlled low-cycle fatigue behavior at 538°C to evaluate the effect of hold periods in tension and in compression .

All the tensile and fatigue tests were performed in argon using hour-glass-shaped specimens while all the modulus of elasticity measurements were performed in air using cylindrical gage section specimens. A servo-controlled, hydraulically actuated fatigue testing machine was used in all these evaluations and the threaded test specimens were mounted in the holding fixtures of the test machine using special threaded adaptors. For the environmental (argon) tests a specially constructed pyrex containment vessel was positioned between the holding fixtures of the fatigue machine and neoprene low-force bellows at either end provided the seal to enable the desired gas purity levels to be maintained throughout the test. Side outlets (with appropriate seals) on this containment vessel provided entrance ports to accommodate the extensometer arms and special lead-throughs near the bottom of the containment vessel enabled the thermocouples, used for specimen temperature measurement, to be routed out to the temperature control system. Specimen test temperatures were attained using induction heating and this was provided by winding a closely spaced induction coil around the outer surface of the cylindrical containment vessel (see Figure 1).

All force measurements were made using a load cell mounted within the loading train of the fatigue machine and specimen strains were measured using specially designed, high temperature extensometers. For the short-term tensile and fatigue evaluation a diametral extensometer was employed while an axial extensometer was used in the modulus of elasticity determinations. A special test procedure was developed to allow the short-term tensile tests to be performed at a constant strain rate which was maintained throughout the test. In the fatigue tests an analog strain computer was employed which allowed the diametral strain signal to be used in conjunction with the load signal so as to provide an instantaneous value for the axial strain which was then the controlled variable. When the modulus measurements were made the axial extensometer was attached to the cylindrical test specimen (gage length of 1.27 cm) and then the specimen was loaded within the elastic region while a plot was made of the corresponding load and axial strain information. A slope calculation of this record yielded the desired modulus value.

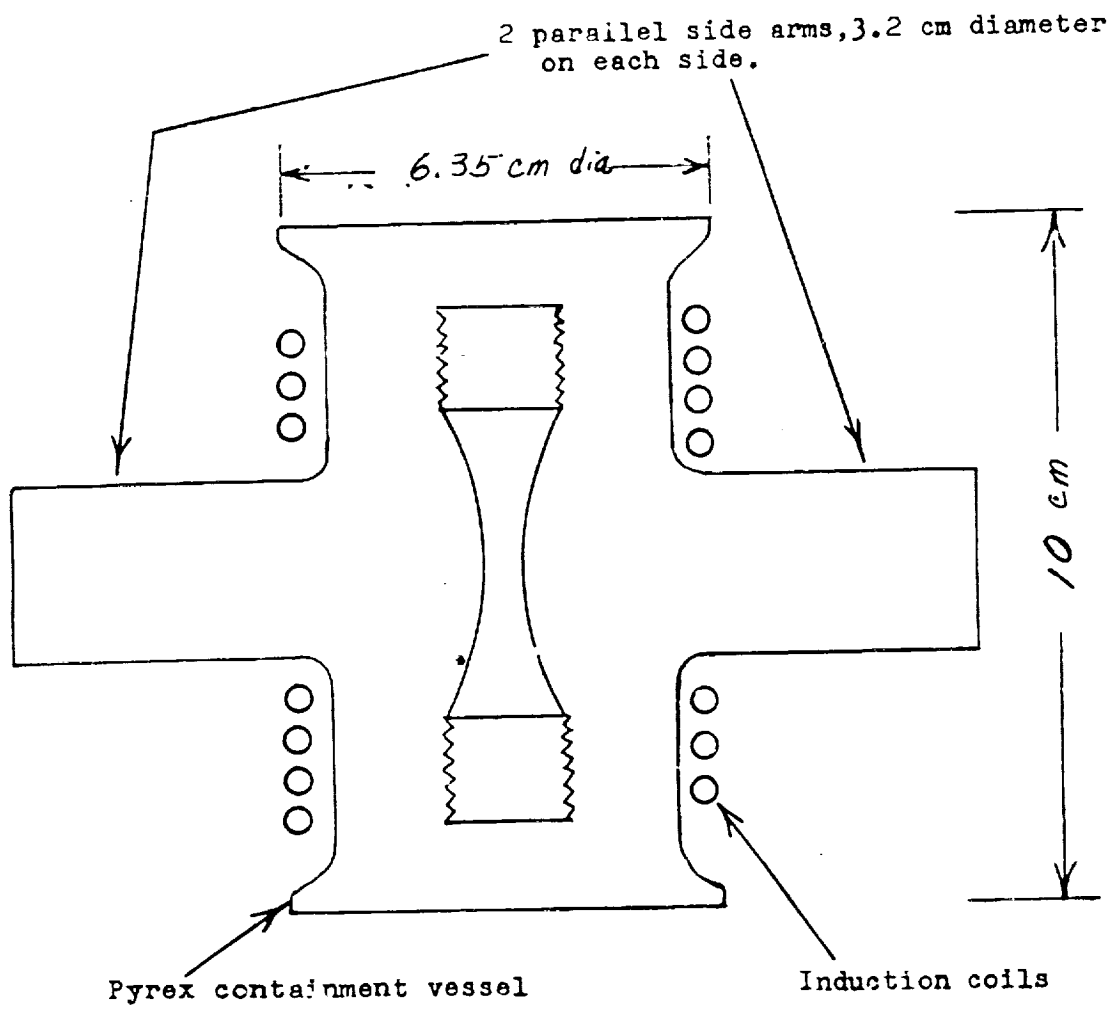The studies performed in this Task 2 effort to define

Figure 1- Schematic of Pyrex Environmental Test Chamber.

temperature, strain-rate and hold-time effects yielded some important information for the R-2 alloy. Some general observations of special interest include:

1) the 0.2% yield strength and ultimate tensile strength of the R-2 alloy decrease gradually with increasing temperature and vary from about 340 and 380 $MN/m^2$ respectively at room temperature to about 150 and 160 $MN/m^2$ at 593°C; the reduction in area increases gradually to about 90% as the temperature is increased to 593°C;

2) the tensile properties of the material were not significantly affected by strain rate at 538°C over the range from $4 \times 10^{-4}$ to $1 \times 10^{-2}$ $sec^{-1}$;

3) the modulus of elasticity decreased from about 115,000 to 70,000 $MN/m^2$ over the temperature range from room temperature to 593°C;

4) The R-2 alloy exhibited a very decided cyclic strain softening;

5) the fatigue life at a strain rate of $2 \times 10^{-3}$ $sec^{-1}$ was unaffected by temperature over the range from 482° to 593°C;

6) the fatigue life at 538°C was decreased as the strain rate decreased;

7) the fatigue life at 538°C was decreased by hold periods in tension; hold periods in compression exerted essentially no effect on the fatigue life;

8) the amount of stress relaxation which occurred during a tension hold period was the same as that observed in a compression hold period of the same duration;

9) after the first fatigue cycle or so the ratio of the stress decrease due to relaxation to the stress level at the start of the hold period remained essentially constant throughout the test.

## III - MATERIAL AND SPECIMENS

Specimen material for use in this portion of the program was supplied by NASA-Lewis Research Center, Cleveland, Ohio. It was zirconium-copper alloy in the 1/2 hard condition and was designated as the R-2 alloy. This material was purchased from Bridgeport Brass Co. in the form of 1.90 cm diameter round bars, Mill Order 96700 (50% reduction of area plus aged). Nominal composition: (% by Wt.) Zr-.20, Ni-.002, Fe-.002, Cu-balance.
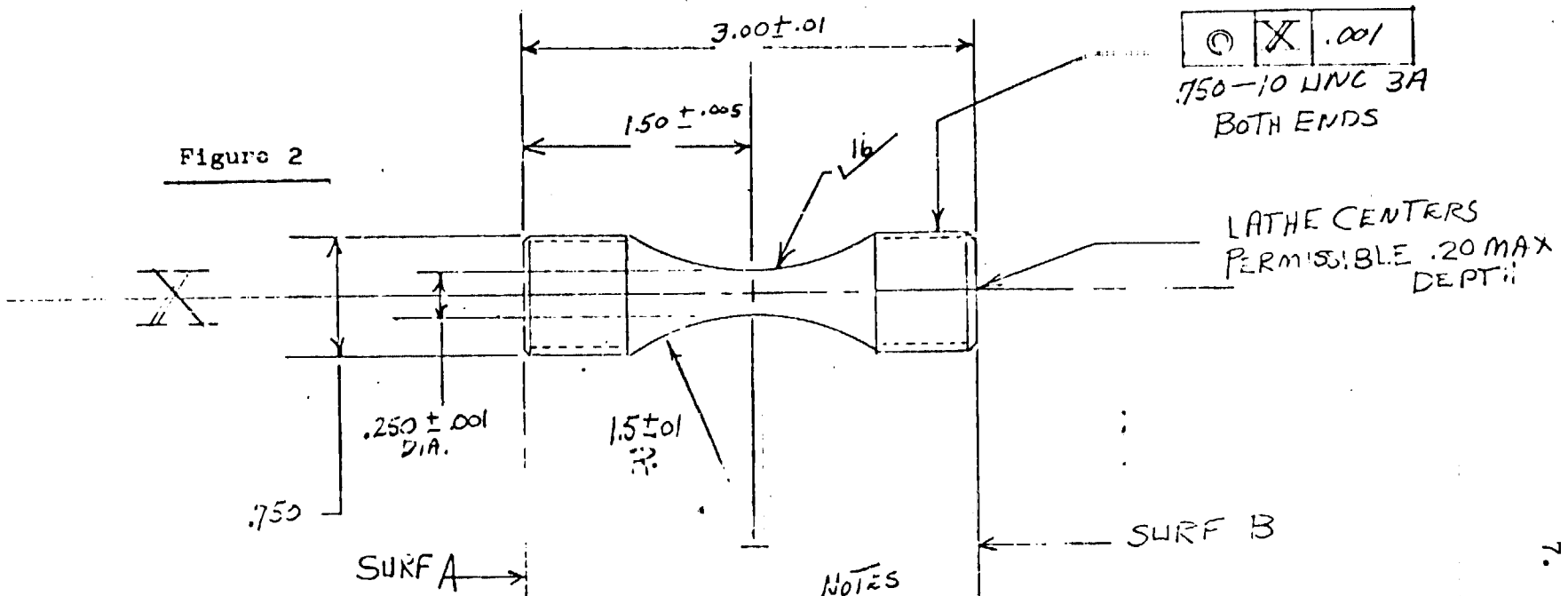
Thirty-eight (38) specimens having the design shown in Figure 2 were fabricated for use in the tensile and fatigue evaluations. In addition, three (3) specimens of the design shown in Figure 3 were machined for use in modulus of elasticity measurements. A photograph of these two types of test specimens is presented in Figure 4.

After being machined, all specimens were wrapped in soft tissue paper and placed in individual hard plastic cylinders (about 9 cm in length and 2.2 cm inside diameter). The ends of these cylinders were then sealed with masking tape and the specimen code number was written on the external surface of the cylinder. These cylinders were used for storage before and after test.

In preparing for a test each specimen was subjected to the following:

1) a small longitudinal notch was filed in the threaded sections of the specimen; this was designed to aid in the removal of entrapped air from the threaded area after the specimen was inserted in the adaptors (see below for specimen-adaptor assembly);
2) the specimen was washed with Freon to remove any surface oils which might have remained after machining;
3) a small quantity of dilute phosphoric acid was applied by hand to the complete surface of the specimen; this removed any surface oxides and any machining oil not removed by the cleaning with Freon; this operation was completed within 15 seconds;
4) the specimen was rinsed in warm water and dried using soft absorbent tissue;
5) the specimen was then subjected to a final cleaning with Freon.

Figure 2

3.00 ± .01

1.50 ± .005

16

.750—10 UNC 3A
BOTH ENDS

⌀ | X | .001

LATHE CENTERS
PERMISSIBLE .20 MAX
DEPTH

.250 ± .001
DIA.

1.5 ± .01
R.

.750

SURF A →

SURF B

5- SCREW THREADS TO BE
AS LISTED IN NBS
HAND BOOK H 28

NOTES

1- SURFACES A, & B TO BE PARALLEL WITHIN .001
2- SURFACES A, & B TO BE PERPENDICULAR TO
   CENTER LINE OF SPECIMEN WITHIN .0005 TIR
3- CONTOURED PORTION OF SPECIMEN TO HAVE
   A ⌵ FINISH OR BETTER. FINISHING SHOULD
   BE IN THE AXIAL DIRECTION USING LOW
   STRESS LAPPING OR POLISHING OPERATION
4- ALL D.T.'S TO BE CONCENTRIC WITHIN .001 TI.

| UNLESS OTHERWISE SPECIFIED DIMENSIONS ARE IN INCHES TOLERANCES ON | DRAWN | | SPECIMEN | Mar-Test inc. |
|---|---|---|---|---|
| FRACTIONS DECIMALS ANGLES<br>±        ±        ± 3/4 | DATE<br>APPD<br>ISSUED | | Low Cycle FATIGUE | CINCINNATI, OHIO |
| ALL SURFACES ⌵ | APPROVED | DATE | | |
| MATERIAL<br>GVT. OR COML TO BE<br>SPECIFIED | ENGR StC | 4-12-71 | | SIZE MTI-1002 |
| | MFG | | | |
| | MATL | | SCALE 1/1   WT ACTUAL | CONT ON SHEET   SH NO. |

Figure 3

SYM. ABOUT ℄

.375 +.005/- 2 PLCS

8/

◎ | X | .001

.750 -10 UNF 3A
BOTH ENDS

.75

.500 +.001
DIA.

16
2 PLCS

0.50 +.010
RADIUS
2 PLCS
SEE NOTE 3

CHAM .03 +.01 X 30° +5°
2 PLCS

1.75 +.005

3.50 +.01

SURF A

SURF B

NOTES

1. SURFACES A · B TO BE
PARALLEL WITHIN .001

2. SURFACES A & B TO BE
PERPENDICULAR TO X
WITHIN .0005 T.I.R

3. RAD. & GAGE SECTION
TO BLEND SMOOTHLY
WITHOUT UNDERCUT

4. ALL DIAS. TO BE CON-
CENTRIC WITHIN .001 TIR.

5. RAD + UNIFORM GAGE SECTION
TO BE FINISHED USING
LOW STRESS GRINDING.
FINAL FINISH SHOULD
BE OBTAINED WITH LAPPING
OPERATION IN THE AXIAL
DIRECTION

8.

| MAR-TEST INC CINTI. OHIO | TEST SPECIMEN — UNIFORM SECTION | ALL SURF: √ UNLESS OTHERWISE INDICATED |
| --- | --- | --- |
| M.T.I — 1010-M1 | SCALE: NONE | WT. — |
| MATERIAL: PER SPEC. | SPEC'N. NOTES | ALL DIMENSIONS ARE IN INCHES |

TENSILE AND FATIGUE MODULUS

Figure 4 - Photograph of the two types of test specimens
used in the Task 2 effort.

IV – TEST EQUIPMENT

A closed-loop, servo-controlled, hydraulically-actuated fatigue machine (see Figure 5) was employed in this program. This machine was equipped with the necessary recorders to provide continuous readouts of the desired test information.

A block diagram of the type of test machine used is presented in Figure 6 . The programmer is a precision solid-state device capable of furnishing all of the required waveform signals necessary to provide the strain or stress values demanded in the test. This signal is compared in the summing network with the strain or stress values actually present at the specimen at any instant of time. Any deviation from the required parameter is sensed by the servo-controller which supplies a correction current signal to the servo-valve which provides the correct hydraulic flow and pressure to the hydraulic actuator. The actuator in turn imparts the necessary displacement and force through the load cell to the specimen. The diametral displacement of the specimen in the gage section is sensed by the extensometer and the motion is imparted to the LVDT (Linear variable displacement transducer) which supplies an electrical signal to the analog computer. The analog computer accepts the instantaneous diametral strain and axial force signals and operates upon them to provide signals representing all of the strain and stress components of interest. Any one of these can be selected for comparison with the programmer signal.

Manufacturer and nomenclature of the various components of the fatigue machines are as follows:
1. Programmer – designed and built by Mar-Test Inc.
2. Servo-controller – designed and built by Mar-Test Inc.
3. Actuator – Universal Fluid Dynamics, Type MDF5-H-BR
4. Servo-valve – Moog, Model 76-101
5. Hydraulic System – Racine, Model PSV-SSC-20GRS
6. Load Cell – Strainsert, Model FFL15U-2SP (K)
7. Induction Generator – Lepel, Model T-2, 5-1-KC-J-BW
8. Extensometer – designed and built by Mar-Test Inc.
   to measure diametral strain
9. LVDT – ATC, Model 6234A05B01XX
10. Analog Strain Computer – designed and built by Mar-Test Inc.
11. Load Frame and Fixtures – designed and built by Mar-Test Inc.

Each fatigue machine consists of a sturdy three-column support system connecting two fixed, horizontal platens. A movable platen operates between the fixed platens and is hydraulically actuated to provide the desired cyclic motion. The movable platen contains three close-tolerance bushings which slide on the chrome-plated support columns to impart extreme rigidity and precise alignment to the system.

The diametral strain at the minimum diameter point of the specimen is measured using a specially constructed diametral extensometer. This device was fabricated from low thermal expansion materials (quartz and invar) to minimize the effects

Figure 5- Fatigue Laboratory at Mar-Test Inc.
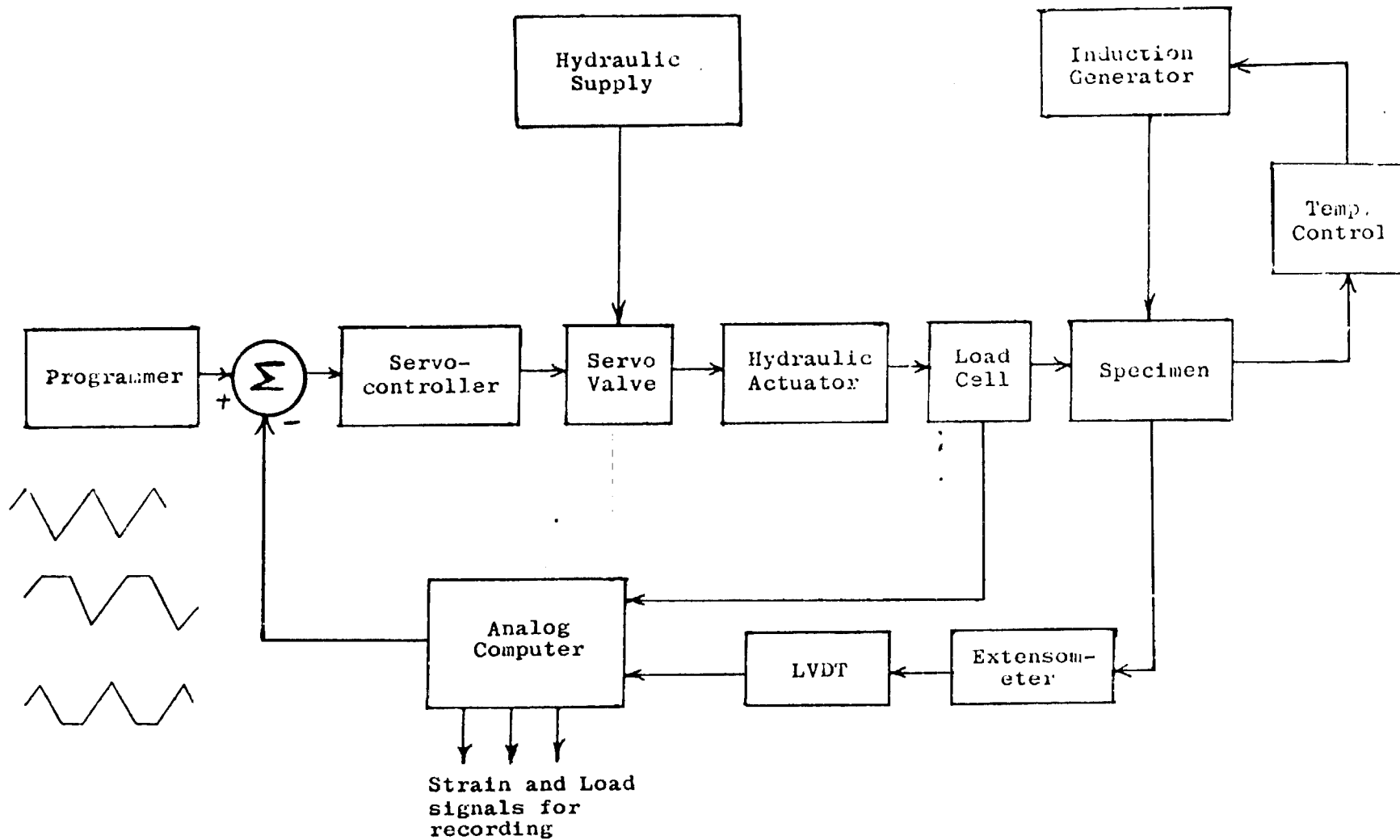Showing Three High Temperature Fatigue
Machines.
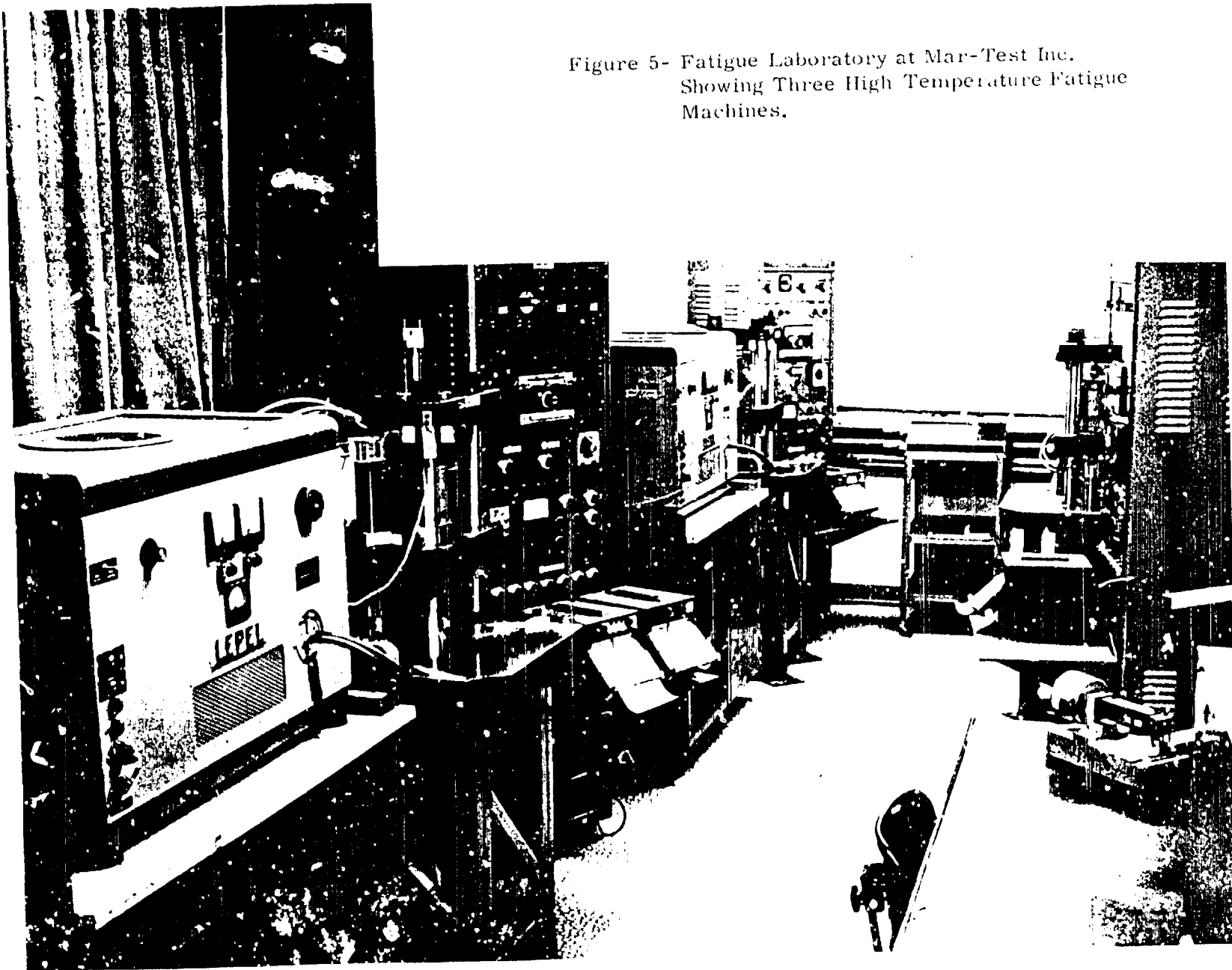
Figure 6 – Schematic of components in fatigue testing machine.

of room temperature changes on extensometer output. Each exten-
someter is calibrated prior to use by employing a special cali-
bration fixture. Each device is supported horizontally (that is,
in the actual use position) with the extensometer knife edges
touching a 0.25 inch diameter split pin. One of the pin halves
is fixed and the other is displaced horizontally to simulate a
diameter increase. This motion is controlled by the rotation of
the barrel of a special micrometer (calibrated against NBS stand-
ard). In this way the extensometer is calibrated to within 10
microinches. With this type of calibration and a knowledge of
the stability and accuracy of the electronic components of the
system a reasonable estimate of the accuracy of the strain con-
trol system is 60 microinches per inch in terms of axial strain
range.

Before any tests are made each load cell is cali-
brated in position by placing a calibrated (NBS) Ring-Force Gauge
(Morehouse Instrument Co., Model 5 BT, 5000 lbs capacity with an
accuracy to 0.2 percent) in the specimen position in the load
train. As the actuator is caused to apply a load the output of
the load cell is plotted against the load indicated by the cali-
brated Ring-Force Gauge. This calibration is performed at fre-
quent intervals to insure accurate stress measurements during
the testing program.

Each fatigue machine has its own control console
which functions to supply the very precise control features
which are so essential to the performance of meaningful fatigue
tests. In addition to housing the temperature controller and an
elapsed time indicator each control console contains:
   a) a calibration panel which also provides means for auto-
      matic or manual control of the hydraulic solenoid and
      power for auxiliary equipment such as the induction
      generator and recorders;
   b) a programmer which provides the required demand signal
      waveform for the test;
   c) an analog strain computer which generates the load and
      strain components for recording and control purposes;
   d) a servo-controller which compares the programmer supplied
      demand signal and the computer supplied feedback signal
      and generates the proper control current for the servo-
      valve; a meter relay circuit operates in conjunction
      with the servo-controller to provide the means for
      shutting down the system when the specimen fails.

One of the important precautionary features of the
Mar-Test fatigue machines is the incorporation of a manually
operated by-pass valve across the hydraulic actuator. With this
valve open the test specimen cannot be exposed to any inadvertent
load transient during start-up. The hydraulic solenoid valve
can be energized with this valve open and the load transients
frequently encountered in test start-up can be eliminated. Once

the solenoid valve is opened the by-pass valve can be closed
slowly to bring the system under control. During this operation
the load trace is monitored so that a smooth transfer is effected
and all load transients are eliminated.

## V - TEST PROCEDURES

### A. Low-Cycle Fatigue

The closed-loop, servo-controlled low-cycle fatigue
machine employed in this study was fitted with a specially con-
structed containment vessel to allow testing in a protective
environment. This cylindrical chamber was fabricated from
2-inch diameter pyrex tubing and was inserted between the hold-
ing fixtures. This small-volume enclosure (about $170 cm^3$) facil-
itated system purging and allowed the desired protective gas
purity levels to be maintained. Neoprene low-force bellows
at the top and bottom connected the chamber to the holding fix-
tures and permitted the normal longitudinal motion of the spec-
imen during cyclic loading. Side-arms on the pyrex containment
vessel provided access for the extensometer arms and a special
flexible joint provided an effective seal without influencing
the strain measurement. Thermocouple lead-throughs were pro-
vided near the lower platen so that the thermocouple leads could
be routed from within the enclosure to the temperature control
system. Specimen heating was effected by an induction coil
wound around the external surface of the cylindrical containment
chamber (see Figure 1).
All the low-cycle fatigue tests in this program were
performed using the specimen configuration shown in Figure 2.
Such specimens were held in specially designed threaded adaptors
to provide an integral assembly that allowed the adaptor to be
heated inductively along with the specimen itself. Large mating
surfaces were provided between the specimen and the adaptors to
minimize the temperature gradient between them. This approach
proved to be quite successful and test temperatures to 593°C
(1100°F) were achieved quite readily. It was also shown that a
very flat longitudinal temperature profile was obtained.

Test temperatures were measured using chromel-alumel
thermocouples spot-welded to the top surface of the bottom adaptor.
Special pre-test calibrations performed in a previous study em-
ployed thermocouples peened into the surface of a copper specimen
and these were used to establish the fact that the temperature of
the adaptor which was in direct contact with the copper specimen
was within 1°C (2°F) of the specimen temperature measured at the
longitudinal midpoint. These tests confirmed the idea that the
temperature of a copper specimen, mounted as described above,
could be accurately measured and controlled through the use of
a thermocouple attached to the adaptor.

Because of the temperature uniformity in the specimen-
adaptor assembly a special precaution must be taken to avoid
failure in the threaded portion of the specimen. This involves
the provision of a large specimen diameter in the grip region
compared to the diameter at the specimen midpoint. This was also

sufficient to avoid plastic deformation at the specimen-adaptor contact point and therefore to prevent backlash and alignment changes during strain cycling.

A fully instrumented test specimen-adaptor assembly was mounted in the holding fixture of the fatigue machine using a split collet type of assembly and a special leveling device was employed to assure that the specimen was installed perpendicular to the platens. A flat load cell (see previous section) in series with the specimen was used to measure the load applied to the specimen throughout the test.

Once the specimen was installed within the containment vessel the system was purged using a high flow rate of high purity argon (see below for inert gas specifications) for 30 minutes. This established the desired purity level within the test chamber. The inert gas flow rate was then lowered to a few $cm^3$/min and maintained at this level throughout the test.

Before any tests were initiated the analog strain computer was calibrated by making use of the specimen cross-sectional area (A) and the value for Young's modulus (E) at the intended test temperature. Modulus values for the two alloys tested were determined in separate tests. The values of A and E were used as shown in the block diagram in Figure 7 to generate axial strain values corresponding to measured values of diametral strain and force. This diagram provides an aid to an understanding of the computer calibration procedure which is based on using the values of A and E and adjusting the compliance control to establish the following equality:

$$A E = F/\mathcal{E}_e$$

Prior to heating a specimen to the desired test temperature the system was placed in force control. This automatically kept the force at zero by gradually lowering the movable platen to account for the thermal expansion of the specimen as the temperature was increased. When test temperature was obtained the analog strain computer was employed to yield a value for Poisson's ratio. The specimen was cycled elastically so that the actual plastic strain, $\Delta \mathcal{E}_p$, was zero and the value of Poisson's ratio could be obtained by the ratio of the diametral to axial strain; thus:

$$\nu_e = \frac{- \mathcal{E}_d}{\mathcal{E}_e}$$

The $\nu_e$ control on the computer was then adjusted to force the computer value of $\Delta \mathcal{E}_p$ to zero. At this point the above relations were satisfied and the correct value of $\nu_e$ was indicated
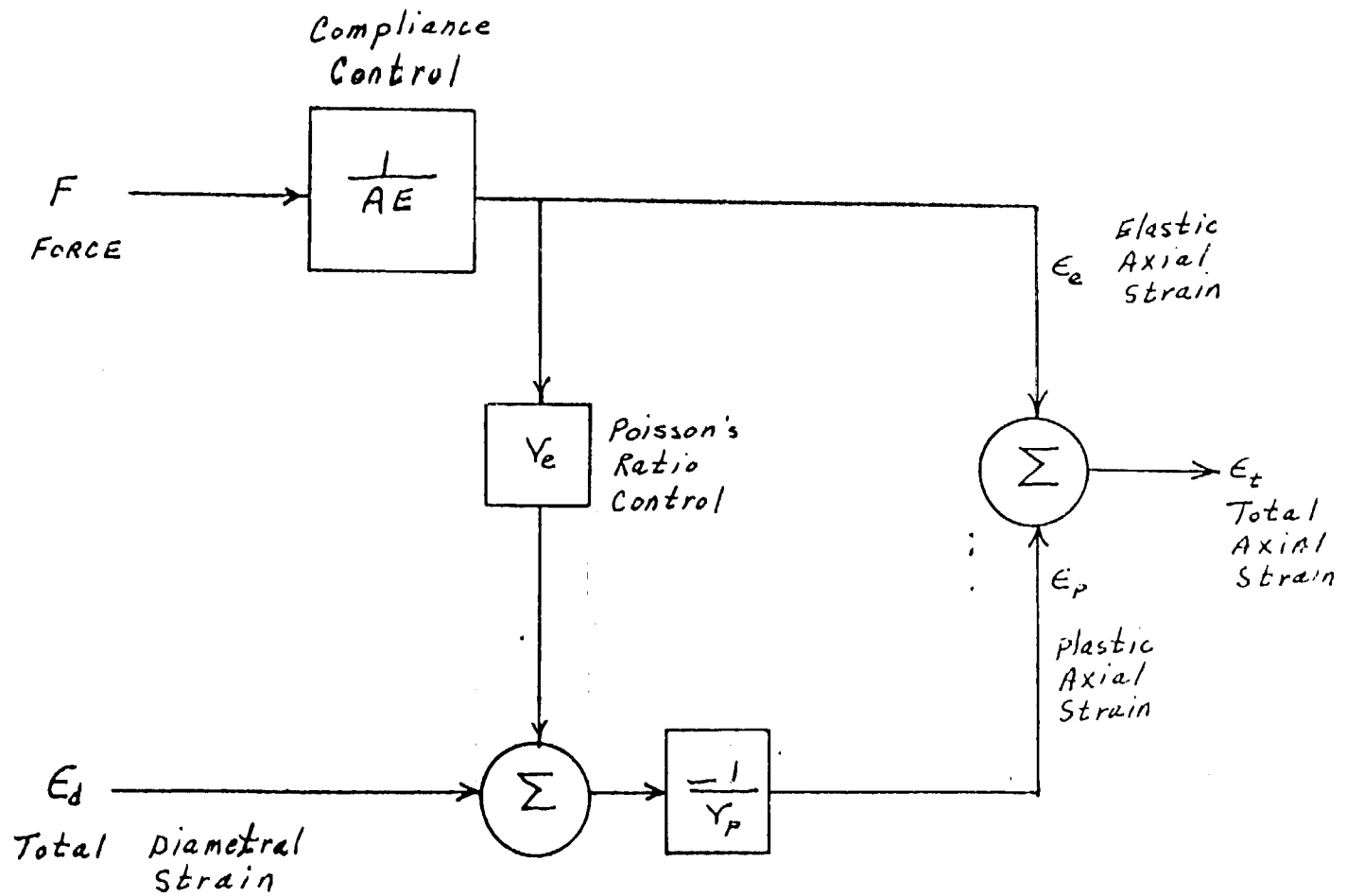
Figure 7- Block Diagram of Strain Computer

on a potentiometer turns-counting dial on the computer panel (the value for Poisson's ratio, plastic, was set internally to 0.5 in accordance with constant volume deformation conditions associated with plastic deformation). At this point the computer was calibrated and furnished a correct axial strain signal for recording and control purposes.

With the computer calibration complete the test was ready to begin. Two recorders were connected to the console, one to monitor load and the other to monitor the total axial strain. The system was placed in automatic control and the strain was gradually increased to the desired level. This gradual increase to the desired strain level requires 5 or 6 cycles and avoids specimen damage due to "overshooting" the strain range which can occur if an attempt is made to impose the desired strain level on the first loading cycle. When the desired strain range was reached the test conditions were kept constant until fracture occurred. Hysteresis loops were recorded on an x-y recorder during the first few cycles and at frequent intervals thereafter. In addition, a continuous recording was made of the applied load and the associated plastic strain. When the specimen fractured, the shut-down circuit automatically de-energized the entire testing system including the induction generator, the hydraulic ram, the timing device and the recorders. However, the protective environment system remained functional until the specimen cooled to room temperature.

High purity (guaranteed 99.999% purity or better) argon gas was employed as the protective environment for the first few tests in the Task 1 portion of this program. It was found, however, that more protection was afforded by the use of a slightly reducing environment which consisted of this same high purity argon gas with an addition of 1000 ppm of hydrogen. This latter environment provided completely satisfactory results for all the high temperature tests of the zirconium-copper alloy specimens. Some indication of the effectiveness of this environment in these tests is provided by the fact that some of the Task 2 tests involved durations close to 60 hours and yet the specimens had a clean and bright appearance at the end of the test. It was not found necessary to employ the tantalum "getter" foil used in some of the Task 1 evaluations.

## B. Short-Term Tensile

Measurements of short-term tensile behavior were made using the same hydraulically-actuated, servo-controlled fatigue machines employed in the low-cycle fatigue evaluations. Furthermore, the same specimen design was employed and the specimen preparation, test environment, installation and instrumentation procedures were identical to those employed in the fatigue tests. These short-term tensile tests were performed using a diametral extensometer and the true diametral strain rate was kept constant at the specified value (the corresponding axial strain rate was about twice this value).

For each test a strip chart recording was made of the measured diametral strain as a function of time and, in addition, an x-y recording was made of the load versus diametral strain. These traces provide test information from the instant of load application all the way to fracture.

## C. Modulus of Elasticity

Modulus of elasticity measurements were made using the same fatigue testing machine employed in the fatigue and tensile evaluations. There were three important differences however. One involved the use of a cylindrical gage section specimen (see Figures 3 and 4) instead of the hourglass-shaped specimen while the second difference involved the use of an air instead of an argon environment. The third difference was associated with the use of an axial rather than a diametral extensometer. This axial extensometer was developed at Mar-Test Inc. for use in some special low-cycle fatigue evaluations of high temperature anisotropic materials which required that the axial strain be both measured and controlled. This device is shown schematically in Figure 8 and is seen to consist of horizontal arms (1.25 cm diameter quartz rods) mounted in the same vertical plane, an elastic (invar) hinge assembly, an LVDT, special quartz tips which contact the cylindrical gage section specimen to identify the gage length, a spring-loaded fixture which maintains the contact between the extensometer tips and the gage section, and a specially designed suspension system which accommodates the axial deflection of the specimen external to the gage section as well as the axial strain which occurs within the gage section. This suspension system also allows the extensometer to move horizontally to follow the diametral changes which take place as the specimen is loaded.

Although the extensometer has a variable gage length feature, a 0.5 inch gage length was established for the modulus measurements. The 0.5 inch gage length was established with a special gage block at room temperature. Use of this device allowed for the definition of the gage length within 0.5 percent. A fixed mechanical reference point was then established for the 0.5 inch gage length and related directly to an electrical reference. With this technique the 0.5 inch gage length could be reproduced independent of the specimen temperature.

Calibration of the extensometer was achieved by suspending and attaching the extensometer to a special calibration fixture to closely simulate the technique employed in an actual test. The rotation of a precision Barrel-type micrometer (containing 0.00001 inch divisions) with a non-rotating head caused a known amount of either positive or negative displacement to occur at the extensometer tips edges. This procedure provided information as to the stability, linearity, hysteresis, repeatability and overall accuracy of the extensometer and control circuitry. A reasonable estimate of the overall accuracy of the strain control system is about 30 micro-inches per inch.
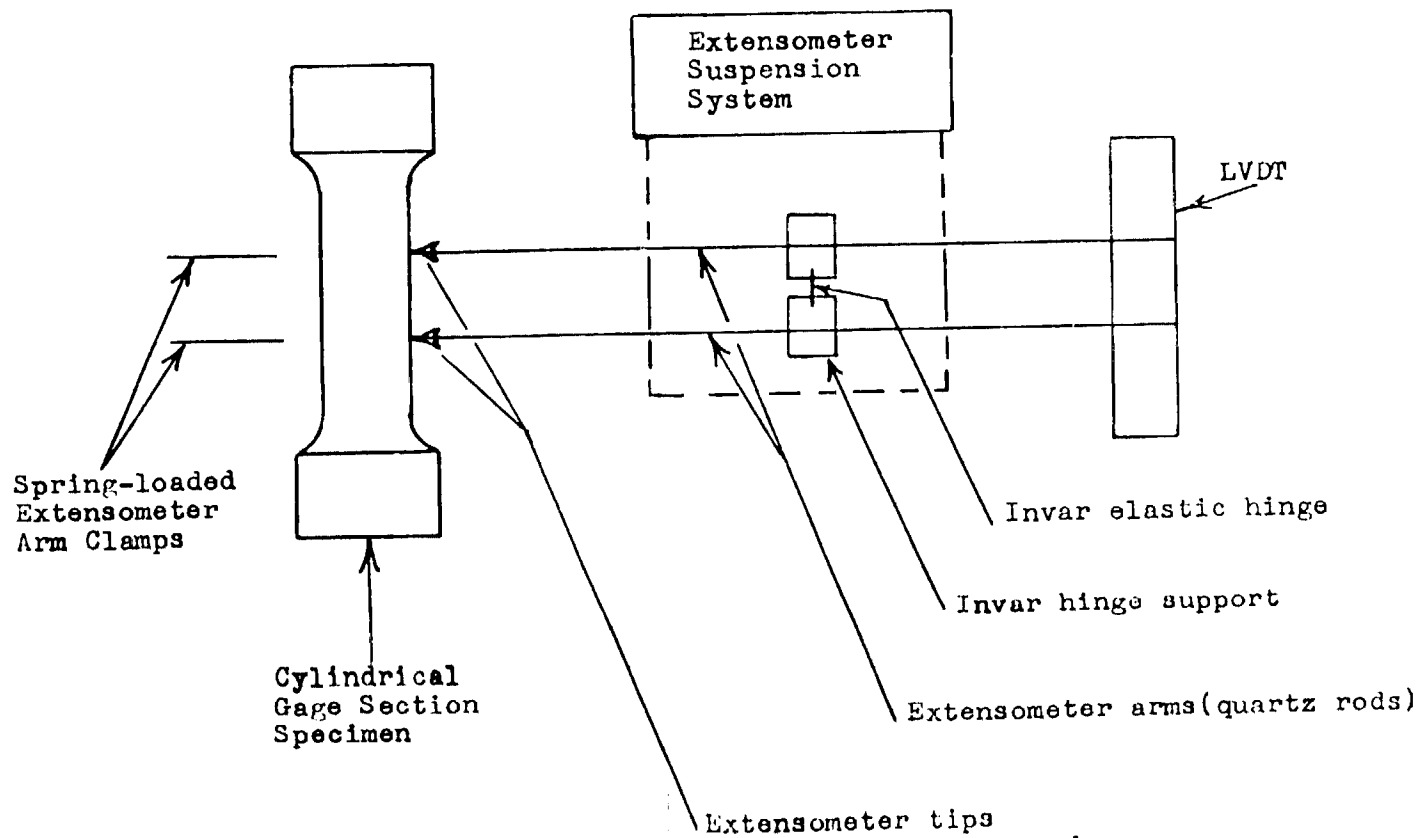
Figure 8- Schematic diagram of axial extensometer used in
Modulus of Elasticity measurements.

Specimen mounting (i.e. using threaded adaptors) and
temperature instrumentation were the same as employed in the ten-
sile and fatigue testing. With the extensometer in place the
specimen was loaded elastically and a continuous trace of the
load versus strain behavior was obtained using an X-Y recorder.
The slope of the line defined on this trace yielded the desired
modulus value for each test temperature.

## VI - TEST RESULTS AND DISCUSSION OF RESULTS

### A - Short-Term Tensile

#### 1. Yield Strength, Ultimate Strength and Reduction in Area

All of the short-term tensile tests were performed in duplicate to yield the results presented in Table 1. In general, the reproducibility of the measured property values was excellent. Agreement between duplicate measurements was well within 10 percent.

Plots showing the effect of temperature on the yield strength, ultimate tensile strength and the reduction in area are presented in Figure 9. The room temperature and 538°C data are included to provide a comparison over the entire temperature range covered in this program. A gradual decrease in yield and ultimate strength is indicated as the temperature is increased to 593°C. A slight increase (about 10 percent of the room temperature value) in the reduction in area is noted over this same temperature regime.

A limited assessment of the effect of strain rate on the short-term tensile properties was performed at 538°C. These data are listed in Table 1 and are presented graphically in Figure 10. In general, a slight increase in yield strength, ultimate strength and reduction in area is noted as the strain rate is increased from $4 \times 10^{-4}$ to $1 \times 10^{-2}$ sec$^{-1}$.

#### 2. Modulus of Elasticity

Measurements of the modulus of elasticity were made in air to yield the results presented in Table 2. Here again duplicate tests resulted in excellent reproducibility as the measurements from one specimen to another agreed within a few percent.

A plot showing the modulus of elasticity data at the various test temperatures is presented in Figure 11.

### B - LOW-CYCLE FATIGUE

#### 1. Temperature Effects

It was the intent in this phase of the program to identify the fatigue life at 482° and 593°C using the strain ranges corresponding to 300- and 3000- cycle life as determined in the Task 1 tests at 538°C. As this testing began at 482°C for the R-2 alloy it was found that the 300-cycle strain range of 6.1 percent from the Task 1 results, yielded a fatigue life which was lower than expected. It was decided, therefore, to continue the testing using a strain range of 5.0 percent to evaluate the fatigue behavior in the lower-life region.

TABLE 1 - Short-Term Tensile Properties of R-2 (Zr-Cu, 1/2 Hard) Alloy
Measured in Argon

Diametral Extensometer — Hourglass-Shaped Specimens

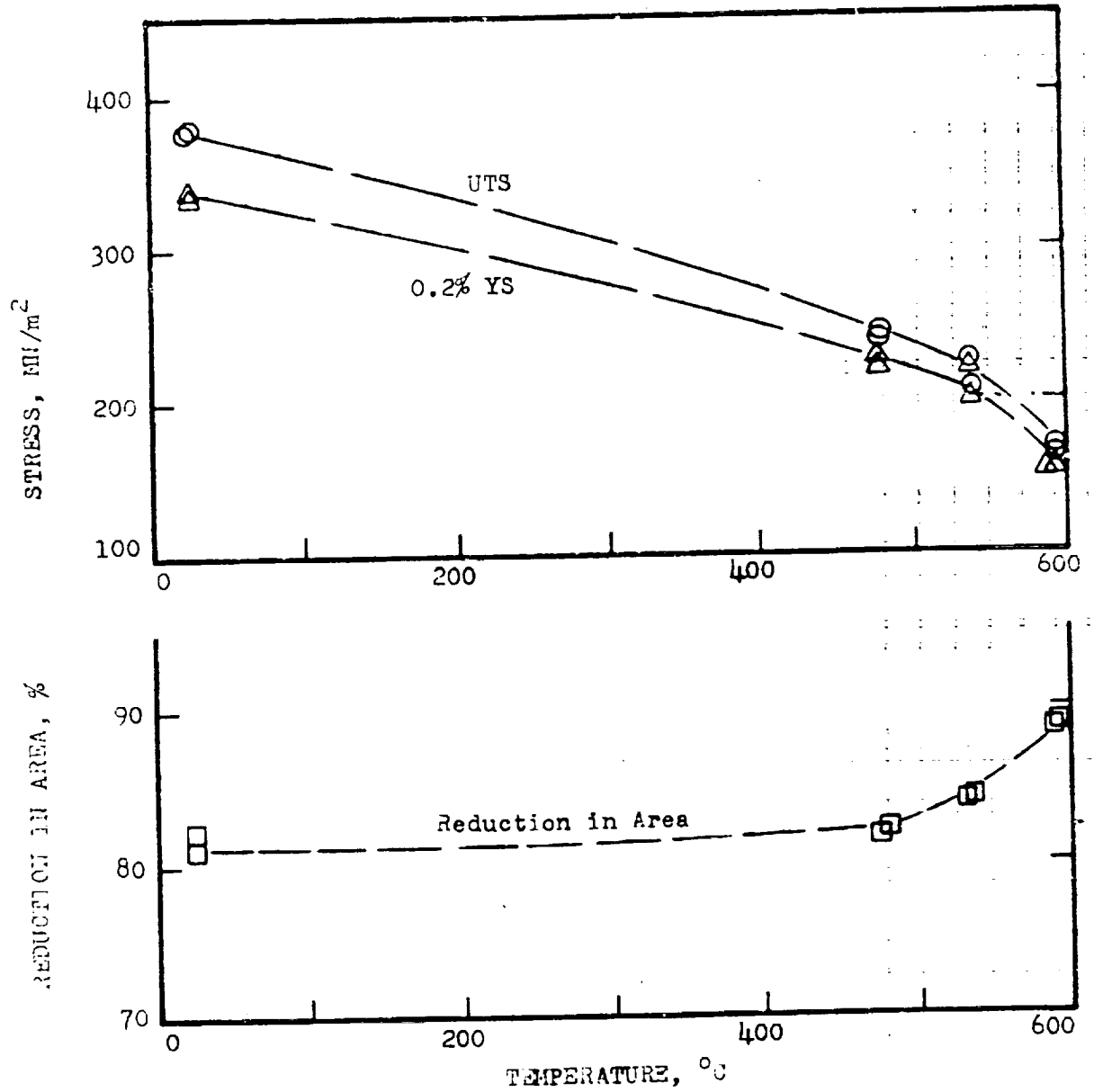| Spec. No. | Temp., °C | Strain Rate, sec$^{-1}$ | 0.2% Offset Yield Strength, MN/m$^2$ | Ultimate Tensile Strength, MN/m$^2$ | Reduction in Area, % |
|---|---|---|---|---|---|
| R-2-18 | 482 | $2 \times 10^{-3}$ | 222.0 | 240.5 | 82 |
| R-2-19 | 482 | $2 \times 10^{-3}$ | 229.0 | 242.5 | 82 |
| R-2-20 | 593 | $2 \times 10^{-3}$ | 156.5 | 168.5 | 89 |
| R-2-21 | 593 | $2 \times 10^{-3}$ | 156.5 | 165.0 | 89 |
| R-2-22 | 538 | $1 \times 10^{-2}$ | 211.0 | 225.5 | 86 |
| R-2-23 | 538 | $1 \times 10^{-2}$ | 203.5 | 225.0 | 85 |
| R-2-24 | 538 | $4 \times 10^{-4}$ | 182.5 | 185.0 | 84 |
| R-2-25 | 538 | $4 \times 10^{-4}$ | 182.5 | 198.0 | 79 |

Figure 9 – Short-Term Tensile Properties at Various Temperatures for Zirconium-Copper Alloy (1/2 Hard) Tested in Argon using a strain rate of $2 \times 10^{-3}$ sec$^{-1}$ (Data at RT and 538°C are taken from Task 1 Results

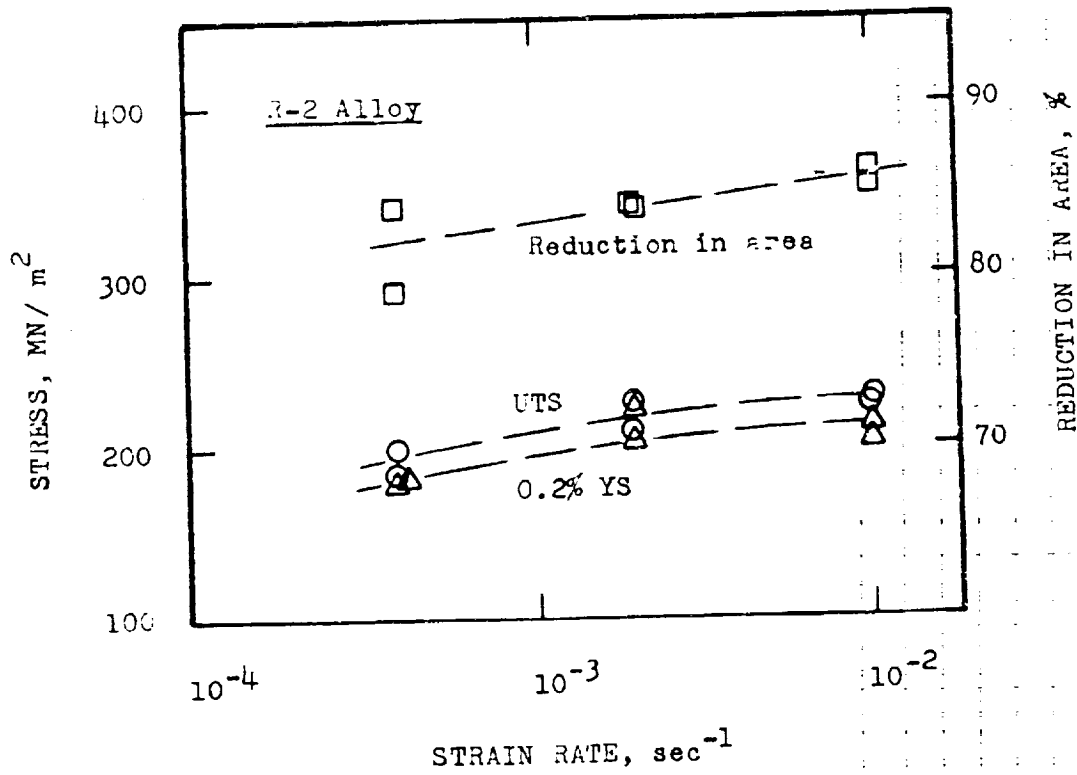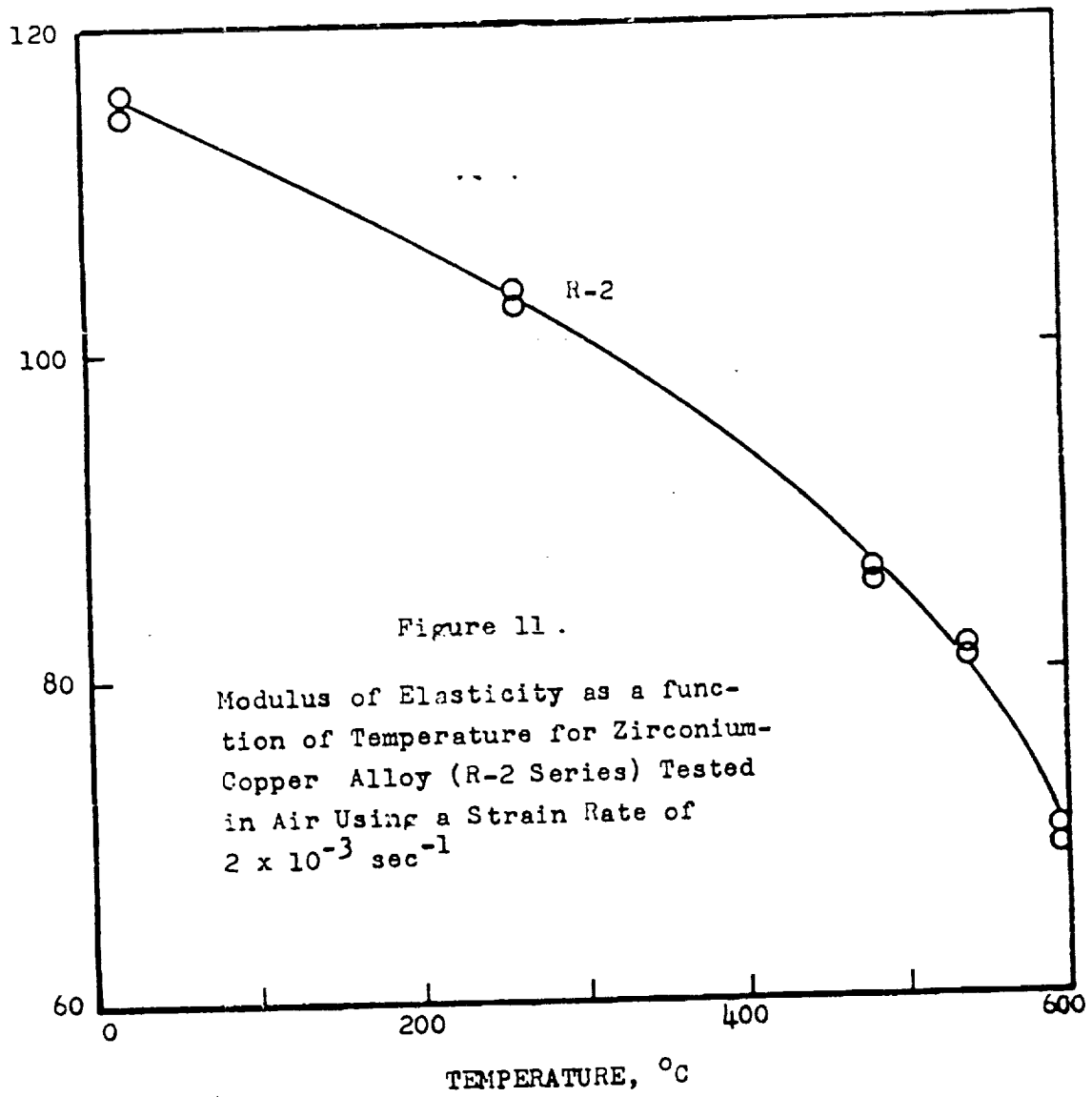Figure 10 - Effect of Strain Rate on Short-Term Tensile
Properties of Zirconium-Copper Alloy (1/2 Hard)
and Narloy Z Alloy at $538^{\circ}C$
(Data at $2 \times 10^{-3}$ sec$^{-1}$ for R-2 are taken from
Task 1 results)

| Table 2 - Modulus of Elasticity Values for R-2 (Zr - Cu, 1/2 Hard) Alloy Tested in Air Using a Strain Rate of $2 \times 10^{-3} \text{ sec}^{-1}$ | | |
|---|---|---|
| Axial Extensometer | Cylindrical Gage Section Specimen | |
| Temp., °C | Modulus of Elasticity, $\text{MN/m}^2$ | |
| | Spec. No. R-2-15 | Spec. No. R-2-16 |
| 93 | $116.0 \times 10^3$ | $114.5 \times 10^3$ |
| 260 | $102.7 \times 10^3$ | $103.7 \times 10^3$ |
| 482 | $85.4 \times 10^3$ | $86.3 \times 10^3$ |
| 538 | $80.6 \times 10^3$ | $81.4 \times 10^3$ |
| 593 | $68.95 \times 10^3$ | $70.4 \times 10^3$ |

Figure 11.

Modulus of Elasticity as a function of Temperature for Zirconium-Copper Alloy (R-2 Series) Tested in Air Using a Strain Rate of $2 \times 10^{-3}$ sec$^{-1}$

A summary of the low-cycle fatigue results obtained in this portion of the program is presented in Table 3. In these compilations the modulus of elasticity values which were used in the computer calibration at each temperature are listed and were derived from the actual modulus measurements made in another portion of this Task 2 effort. Also included in these tables are:

a) the value of Poisson's ratio measured in each test
b) the total axial strain range
c) the stress range observed at the start of the test
d) the stress range, plastic strain range and elastic strain range observed a point in the test corresponding to one-half of the fatigue life (i.e. $N_f/2$)
e) the fatigue life, $N_f$

and

f) an indication of whether cyclic strain hardening or cyclic strain softening was observed.

A logarithmic plot of the total strain range versus cycles to failure is presented in Figure 12. Also included in this figure for comparative purposes is a faired curve for the R-2 alloy which was identified at 538°C in Task 1. No noticeable temperature effect is indicated as the fatigue life appears to be essentially the same at 482° and 593°C. There is an apparent discrepancy in the high strain range region where the data at 482°C and 593°C indicate a lower fatigue life than that defined by the curve at 538°C. It is felt, however, that this is not a real difference and arises because the curve at 538°C was positioned with only a limited number of test points in the high strain ranges. This conclusion is supported by the plot shown in Figure 13 based on the R-2 test points at 538°C from Task 1 and those obtained for this material at 482° and 593°C in the Task 2 tests. It seems clear from this plot that a more representative curve for the zirconium-copper (1/2 hard) alloy is obtained when all these results are considered together. This plot in Figure 13 also supports the conclusion that the data at all three temperatures define essentially the same behavior within a fairly narrow scatter band.

## 2. Strain-Rate Effects

Low-cycle fatigue tests were performed in argon at 538°C using strain rates of $4 \times 10^{-4}$ sec$^{-1}$ and $1 \times 10^{-2}$ sec$^{-1}$ with the results shown in Table 4. These data are presented graphically in Figure 14 to indicate a definite strain-rate effect. As the strain rate is decreased the creep effect becomes more prominent and is evidenced by a reduction in the fatigue life.

## 3. Hold-Time Effects

An evaluation of the effect of hold periods (at peak strain) on fatigue life was performed in argon at 538°C. In these tests, two different strain ranges were employed and the cycling rate, exclusive of the hold period, was always $2 \times 10^{-3}$ sec$^{-1}$. Hold period durations were set equal to four times the

## Table 3 - Low-Cycle Fatigue Test Results Obtained in Argon Using a Strain Rate of $2 \times 10^{-3}$ sec$^{-1}$

**R-2 Series**
**Zirconium Copper; 1/2 Hard**

**Axial Strain Control**
**A - Ratio of infinity**

| Spec. No. | Poisson's Ratio | Total Strain Range, % | Stress Range at Start, MN/m$^2$ | at N$_f$/2 | | | N$_f$, Cycles to Failure | Remarks |
|---|---|---|---|---|---|---|---|---|
| | | | | $\Delta\epsilon_p$, % | $\Delta\epsilon_e$, % | $\Delta\sigma$, MN/m$^2$ | | |
| 482°C; E = 85.5 × 10³ MN/m² | | | | | | | | |
| R-2-26 | 0.34 | 6.1 | 472 | 5.8 | 0.3 | 257 | 204 | softened |
| R-2-27 | 0.33 | 1.41 | 483 | 1.16 | 0.242 | 207 | 2,985 | softened |
| R-2-28 | 0.335 | 6.1 | 496 | 5.8 | 0.31 | 265 | 176 | softened |
| R-2-29 | 0.335 | 1.41 | 482 | 1.16 | 0.26 | 221 | 2,135 | softened |
| R-2-30 | 0.34 | 5.0 | 468 | 4.72 | 0.28 | 241 | 265 | softened |
| 593°C; E = 68.95 × 10³ MN/m² | | | | | | | | |
| R-2-31 | 0.32 | 1.4 | 283 | 1.28 | 0.131 | 90.4 | 3,380 | softened |
| R-2-32 | 0.33 | 5.0 | 283 | 4.83 | 0.153 | 105.5 | 346 | softened |
| R-2-33 | 0.33 | 1.5 | 303 | 1.37 | 0.14 | 96.5 | 2,008 | softened |
| R-2-34 | 0.33 | 5.0 | 317 | 4.9 | 0.175 | 120 | 234 | softened |
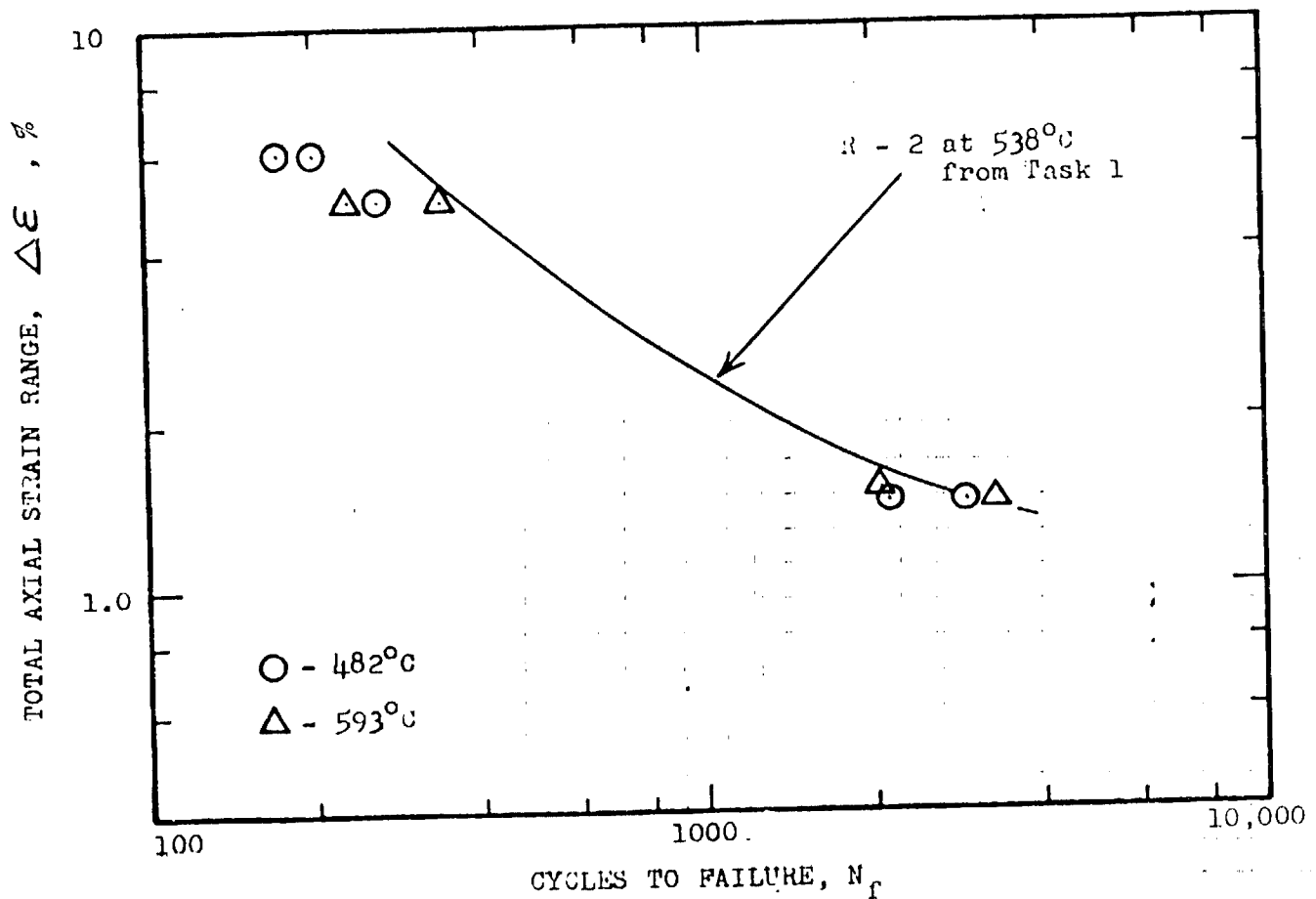
Figure 12 - Fatigue life versus strain range data for Zirconium-Copper alloy tested at 482° and 593°C in argon using a strain rate of $2 \times 10^{-3}$ sec$^{-1}$
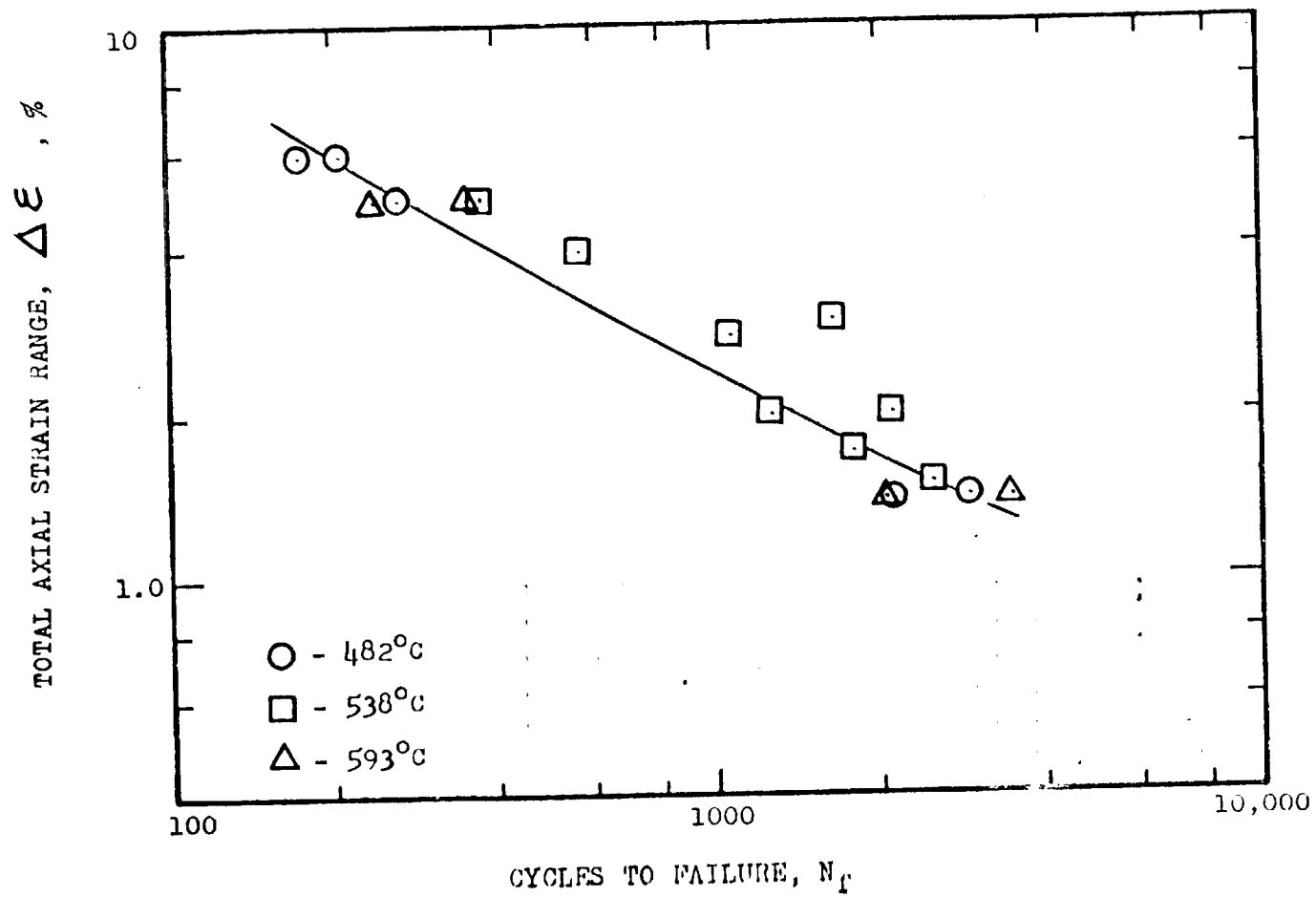
Figure 13- Composite plot of fatigue life versus total strain range for Zirconium-Copper alloy tested in arrow 482°, 538° and 593°C using a strain rate of $2 \times 10^{-3}$ sec$^{-1}$.

R— 2 Series
Zirconium Copper; 1/2 Hard

Axial Strain Control
A - Ratio of infinity
$E = 80.7 \times 10^3$ MN/m$^2$

| Spec. No. | Poisson's Ratio | Total Strain Range, % | Stress Range at Start, MN/m$^2$ | at $N_f/2$ $\Delta\epsilon_p$, % | at $N_f/2$ $\Delta\epsilon_e$, % | at $N_f/2$ $\Delta\sigma$, MN/m$^2$ | $N_f$, Cycles to Failure | Remarks |
|---|---|---|---|---|---|---|---|---|
| Strain Rate = $4 \times 10^{-4}$ sec$^{-1}$ | | | | | | | | |
| R-2-36 | 0.34 | 5.0 | 331 | 5.0 | 0.14 | 113 | 234 | softened |
| R-2-37 | 0.35 | 1.4 | 345 | 1.28 | 0.13 | 103.5 | 1,613 | softened |
| R-2-39 | 0.35 | 5.0 | 324 | 4.84 | 0.14 | 110.5 | 238 | softened |
| R-2-40 | 0.35 | 1.4 | 351 | 1.30 | 0.12 | 96.4 | 3,693 | softened |
| Strain Rate = $1 \times 10^{-2}$ sec$^{-1}$ | | | | | | | | |
| R-2-35 | 0.34 | 5.0 | 427 | 4.8 | 0.28 | 227 | 245 | softened |
| R-2-38 | 0.35 | 1.4 | 414 | 1.23 | 0.16 | 129 | 5,431 | softened |
| R-2-41 | 0.35 | 1.4 | 400 | 1.22 | 0.155 | 125.5 | 5,215 | softened |
| R-2-42 | 0.35 | 5.0 | 393 | 4.72 | 0.20 | 162 | 462 | softened |
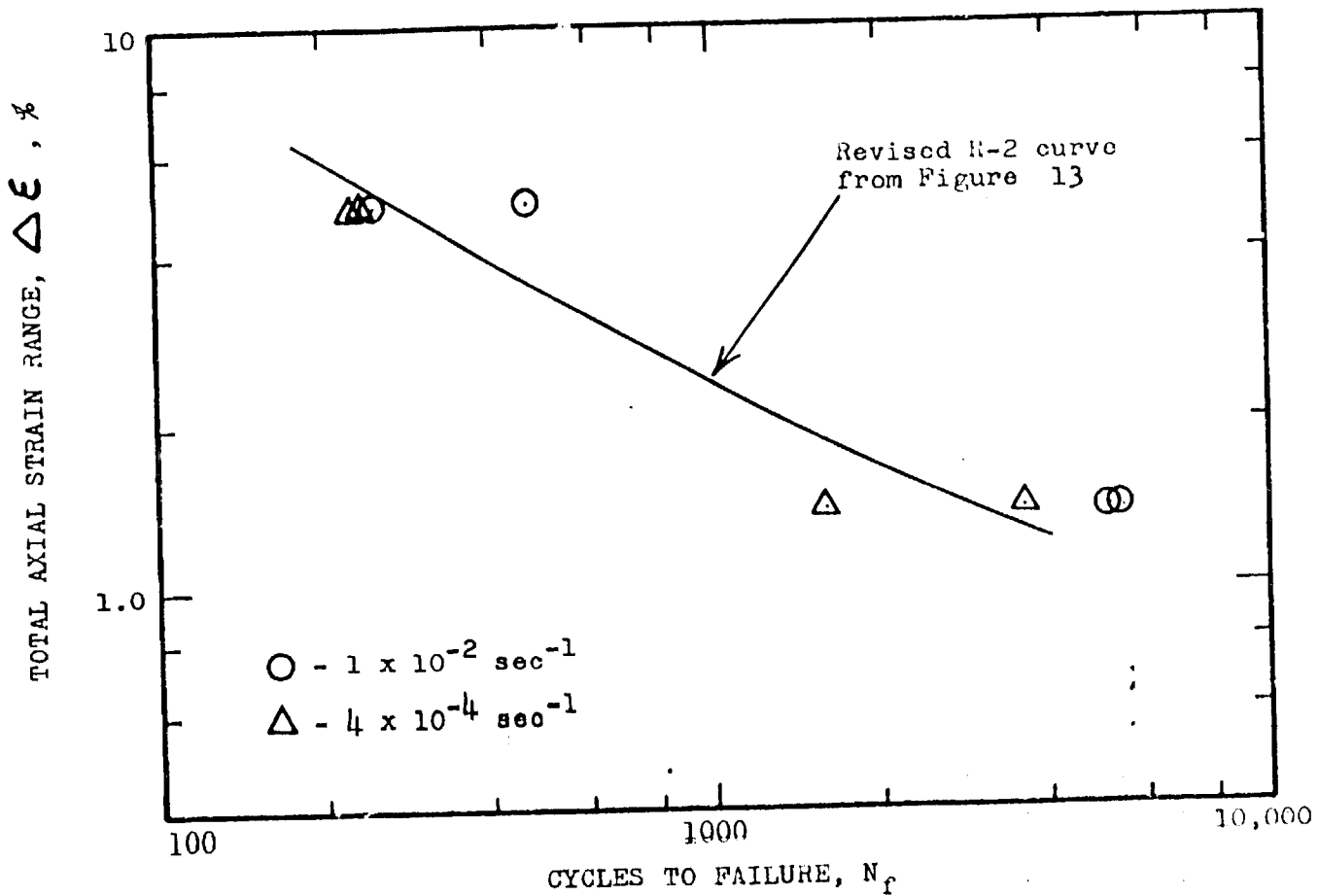
Figure 14 - Fatigue life versus total strain range data for Zirconium-Copper alloy tested at 538°C in argon using strain rates of $4 \times 10^{-4}$ and $1 \times 10^{-2}$ sec$^{-1}$

The chart shows:
- Y-axis: TOTAL AXIAL STRAIN RANGE, $\Delta \epsilon$, %  (from 1.0 to 10)
- X-axis: CYCLES TO FAILURE, $N_f$  (from 100 to 10,000)
- Revised R-2 curve from Figure 13
- Legend: O - $1 \times 10^{-2}$ sec$^{-1}$; $\triangle$ - $4 \times 10^{-4}$ sec$^{-1}$

cycle time corresponding to a continuous cycling test at the given range and a strain rate of $2 \times 10^{-3}$ sec$^{-1}$.

Hold-period durations (in seconds) for these evaluations were calculated using the following expression which applies to the actual strain-time wave form employed:

$$\text{Hold-Period Duration (seconds)} = \frac{2 \Delta \varepsilon}{\dot{\varepsilon}_t}$$

where $\Delta \varepsilon$ is the total strain range in cm/cm and $\dot{\varepsilon}_t$ is the strain rate in sec$^{-1}$. The cycling or ramp time for these tests is, of course, equal to one-fourth of this value.

Hold periods in the tension portion of the cycle were evaluated first and, then, duplicate tests were performed except that the hold period was inserted in the compression portion of the cycle. All of the test results obtained in these studies are summarized in Table 5. In addition to the value for the fatigue life and the observation relating to whether the material exhibited cyclic strain hardening or strain softening, each test is listed with the results obtained in an evaluation of the material characteristics at a point corresponding to one-half the fatigue life (i.e. at $N_f/2$). This information includes stress range ( $\Delta\sigma$ ), maximum tensile stress ( $\sigma_t$ ), maximum compressive stress ( $\sigma_c$ ), the value of the relaxed stress at the end of the hold period ( $\sigma_r$ ), the amount of stress relaxation observed in the hold period ( $R_\sigma$ ), and the various strain components.

A graphical presentation of the fatigue life data is shown in Figure 15 along with the curves established in Figure 13. It is clear that at 538°C hold periods in compression have no effect on the fatigue life of the R-2 alloy. This plot also makes it clear that hold periods in tension have a much more detrimental effect on fatigue life than hold periods in compression. Another observation relates to the fact that the tension hold-time effect appears to become more pronounced as the strain range is decreased despite the fact that the actual hold time is less. A final observation relates to a comparison between the tension hold-time results and the results obtained at a strain rate of $4 \times 10^{-4}$ sec$^{-1}$ (from Figure 14). In both types of evaluation the cycle time (duration of one cycle) was the same but in all cases the cyclic life observed in the hold-time tests was always lower (only slightly at the higher strain ranges but very noticeably in the lower strain range region) than that obtained in the slow strain rate tests. This, of course, indicates a slightly higher creep damage effect in the tensile hold-time evaluations. This behavior is consistent with what many investigators have found for other materials and fits the pattern expected by the strain range partitioning approach of NASA-Lewis Research Center.

Table 5 - Low-Cycle Fatigue Results Obtained in Hold-Time Tests In Argon at 538°C Using a Ramp Strain Rate of $2 \times 10^{-3}$ sec$^{-1}$

R-2 Series
Zirconium Copper (1/2 Hard)

Axial Strain Control
A - Ratio of infinity
$E = 80.7 \times 10^3$ MN/m$^2$

| Spec. No. | Poisson's Ratio | Total Strain Range, % | Cycling Data | | $N_f$, cycles to failure | Remarks |
|---|---|---|---|---|---|---|
| | | | Ramp Time, sec | Hold Time, sec. | | |
| R-2-43 | 0.35 | 5.0 | 50 | 200, Tension | 211 | softened |
| R-2-44 | 0.35 | 5.0 | 50 | 200, Tension | 190 | softened |
| R-2-45 | 0.35 | 5.0 | 50 | 200, Compression | 253 | softened |
| R-2-46 | 0.35 | 5.0 | 50 | 200, Compression | 262 | softened |
| R-2-47 | 0.355 | 1.4 | 14 | 56, Tension | 1152 | softened[*] |
| R-2-48 | 0.35 | 1.4 | 14 | 56, Tension | 1062 | softened[*] |
| R-2-49 | 0.35 | 1.4 | 14 | 56, Compression | 1947 | softened; extensive barrelling |
| R-2-50 | 0.35 | 1.4 | 14 | 56, Compression | 3180 | softened; extensive barrelling |

[*]Dimensional instability; see Figure 19

Table 5 (contd.) - Low-Cycle Fatigue Results Obtained in Hold-Time Tests in Argon at 538°C Using a Ramp Strain Rate of 2 x 10$^{-3}$ sec$^{-1}$

R-2 Series
Zirconium Copper (1/2 Hard)

Axial Strain Control
A - Ratio of infinity
E = 80.7 x 10$^3$ MN/m$^2$

| Spec. No. | Stress Range at Start, MN/m$^2$ | at $N_f/2$ | | | | | | |
|---|---|---|---|---|---|---|---|---|
| | | $\Delta\sigma$, MN/m$^2$ | $\sigma_t$, MN/m$^2$ | $\sigma_c$, MN/m$^2$ | $\sigma_r$*, MN/m$^2$ | $R_\sigma$, Amount of stress relaxation MN/m$^2$ | $\Delta\epsilon_p$, % | $\Delta\epsilon_e$**, % |
| R-2-43 | 372 | 135 | 65.5 | 69.5 | 32.4T | 33.1 | 4.97 | 0.126 |
| R-2-44 | 380 | 152 | 75.8 | 76.2 | 37.9T | 37.9 | 4.95 | 0.142 |
| R-2-45 | 379 | 131 | 63.5 | 67 | 36.5C | 30.5 | 5.0 | 0.124 |
| R-2-46 | 369 | 131 | 62 | 69 | 40.0C | 29 | 5.0 | 0.126 |
| R-2-47 | 379 | 107 | 49.6 | 57.4 | 29.6T | 20 | 1.31 | 0.108 |
| R-2-48 | 379 | 111 | 54.5 | 56.5 | 32.4T | 22 | 1.30 | 0.11 |
| R-2-49 | 382 | 119 | 58.7 | 60.3 | 41.4C | 18.9 | 1.29 | 0.124 |
| R-2-50 | 384 | 125 | 60.8 | 64.2 | 44.1C | 20.1 | 1.28 | 0.13 |

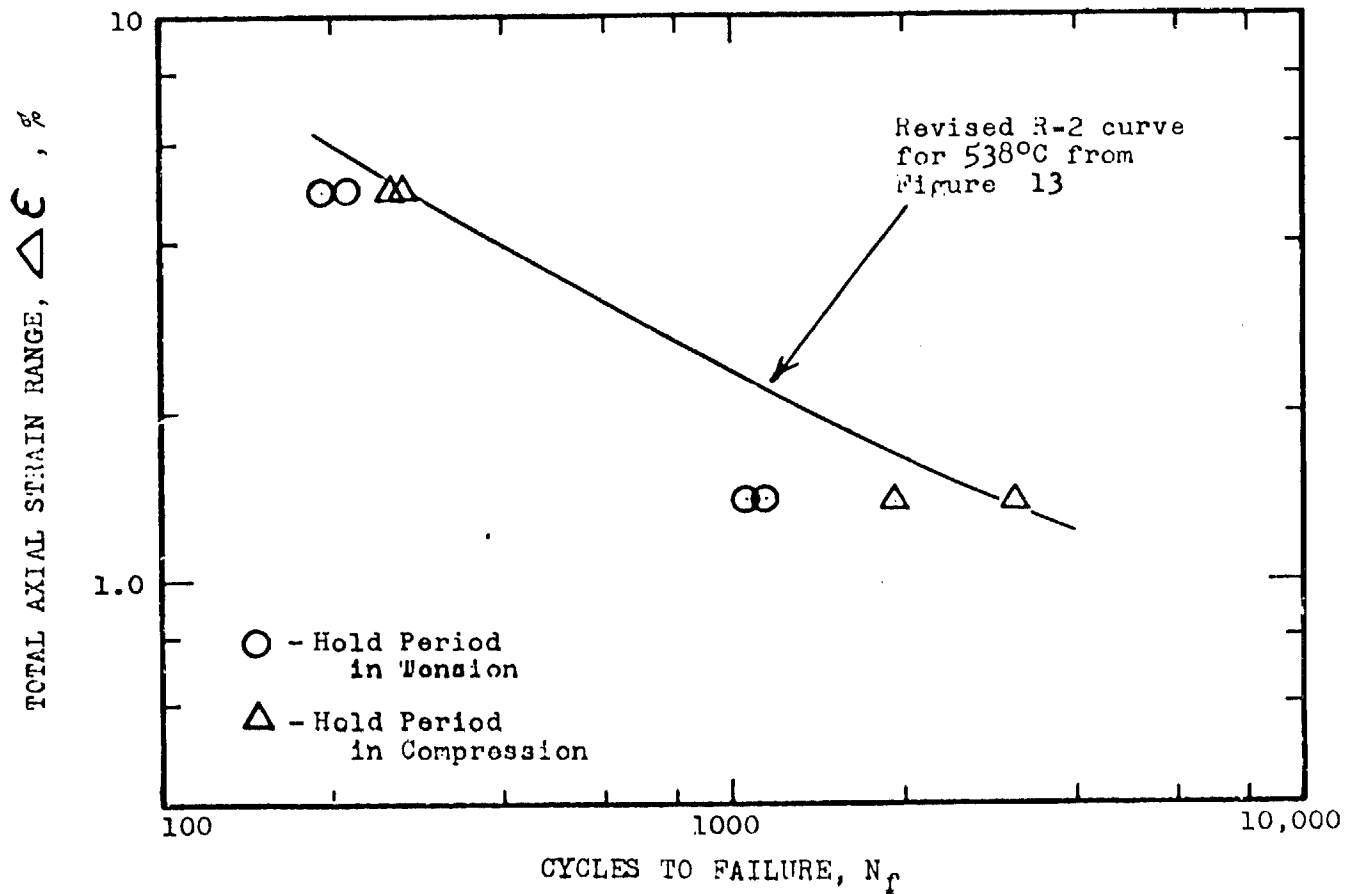*T for tension and C for compression     **Based on relaxed stress range

Figure 15 - Fatigue life versus total strain range for Zirconium-Copper alloy tested at 538°C in argon to evaluate the effect of hold periods

## 4. Relaxation Behavior

Each cycle of a hold-time test provides a brief interval of stress relaxation as the total strain is held constant and the time-dependent conversion of elastic to plastic strain yields a corresponding decrease in stress. This behavior was recorded in the form of continuous load versus time traces to provide a relaxation curve for each cycle. These traces, of course, led to the identification of the $\sigma_t$, $\sigma_c$, $\sigma_r$ and $R_\sigma$ values (at $N_f/2$) mentioned in the previous section.

After the first few hold-time tests were performed it was decided to modify the data recording sequence slightly to allow for the recording of a more detailed relaxation curve. In this modification the speed of the paper drive on the strip chart recorder was increased manually, for one cycle, from the usual value of 0.25 or 0.5 cm per minute to a value of 15 or 30 cm per minute. This manipulation was performed in the range of the tenth cycle and had the objective of providing an expanded relaxation curve to enable the relaxation behavior to be analyzed more easily and the results to be compared from test to test and from material to material.

Since an extensive amount of relaxation information was generated in the hold-time portion of this program some limited assessment of these results was considered to be warranted. One comparison resulting from this evaluation is shown in Figure 16 where the relaxation curves for Spec. Nos. R-2-45 and R-2-46 are presented. Both tests involved a 5.0% strain range with a 200-second hold period in compression and the reproducibility is seen to be very impressive. Also plotted in Figure 16 are some data points taken from the relaxation curve obtained for Spec. No. R-2-44 (5.0% strain range but a 200-second hold period in tension). These points indicate that the relaxation behavior (for the material included and for the test conditions employed) in tension is very similar to that observed in compression. It will be noted that the amount of relaxation obtained after 100 seconds is identical for the tension and compression hold periods. However, it does appear that the tension relaxation within the first second or so is much greater than that in compression. For example, after the first second the tensile stress in Spec. R-2-44 was relaxed by 22.0 MN/m$^2$ whereas in the same time interval the compression stress in Spec. Nos. R-2-45 and R-2-46 had relaxed by only 16 MN/m$^2$.

Another interesting observation evolving from this analysis of relaxation behavior pertains to the amount of relaxation, $R_\sigma$, obtained in each cycle. This quantity was greatest in the first cycle and continuously decreased as cycling progressed although the decrease was very slight beyond the $N_f/2$ point. Decreases in $R_\sigma$ were quite significant and in the R-2-44 test, for example, a value of $R_\sigma$ of 117 MN/m$^2$ was obtained in the first cycle and this decreased to 55 MN/m$^2$ by the eighth
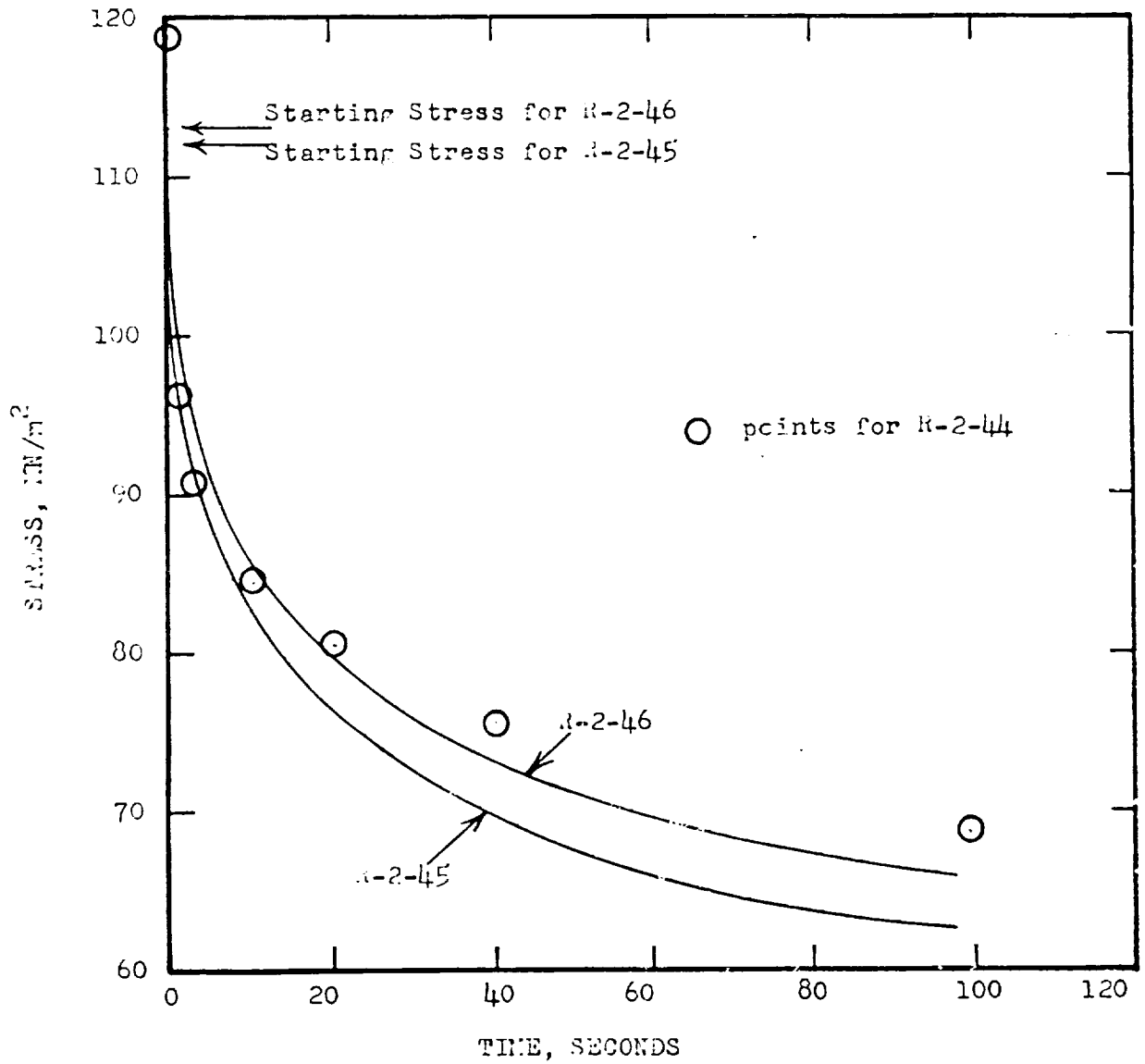
Figure 16 - Typical relaxation data for Zirconium-Copper
(1/2 hard) obtained during the 10th cycle of
a hold-time test in argon at 48°C

cycle. It is interesting to note, however, that after the first cycle or so the ratio of $R_\sigma$ to $\sigma_t$ remained constant throughout essentially the entire test. This ratio was 0.5 in the 5% strain range tests and 0.4 in the 1.4% strain range tests. In other words, even though the $\sigma_t$ value was decreasing because of the cyclic strain softening the amount of relaxation obtained was always (after the first cycle or two) the same fraction of $\sigma_t$. This observation also applies to the relaxation in compression with the use of $\sigma_c$ rather than $\sigma_t$ in the above mentioned ratio.

## 5. Cyclic Stress-Strain Behavior

A brief comparison of the monotonic and cyclic stress-strain behavior is presented in Figure 17. Monotonic behavior was obtained from the stress-strain curves defined in the short-term tensile tests while the cyclic behavior corresponds to the $N_f/2$ data given in Table 3.

These plots emphasize the significant cyclic strain softening that is exhibited by the 1/2-hard zirconium-copper at both 482° and 593°.

## 6. Elastic and Plastic Strain Range Analysis

An analysis of the elastic and plastic strain range data from Table 3 led to the results shown in Figure 18. Linear relations are identified for the elastic and plastic strain components and the slopes of these lines are -0.13 and -0.60 respectively. These values are close to those specified by the Universal Slopes equation.

## 7. Dimensional Instability in R-2 Specimens

During the course of the low-cycle fatigue testing of the R-8 series, R-1 series and R-2 series in the Task 1 portion of this program some of the specimens were found to exhibit a definite dimensional instability referred to as "barrelling", which was most pronounced in the higher ductility materials and in the tests performed at the higher strain ranges. This instability was characterized initially by a deviation from the hour-glass shape as the region at the minimum diameter point tended to become cylindrical. In subsequent stages of this instability the specimen diameter increased noticeably in the regions just above and below the plane of the specimen corresponding to the extensometer location and in certain tests (particularly in the R-8 series described in the Task 1 report) the instability was so severe that the specimen appeared to have a notched configuration. Some instability was again observed in certain tests of the zirconium-copper alloy performed in the Task 2 portion of the program. This instability first became prominent in the high strain range (5%) tests at a strain rate of $4 \times 10^{-4}$ sec$^{-1}$ where the test durations were on the order of 15 hours. It became even more noticeable
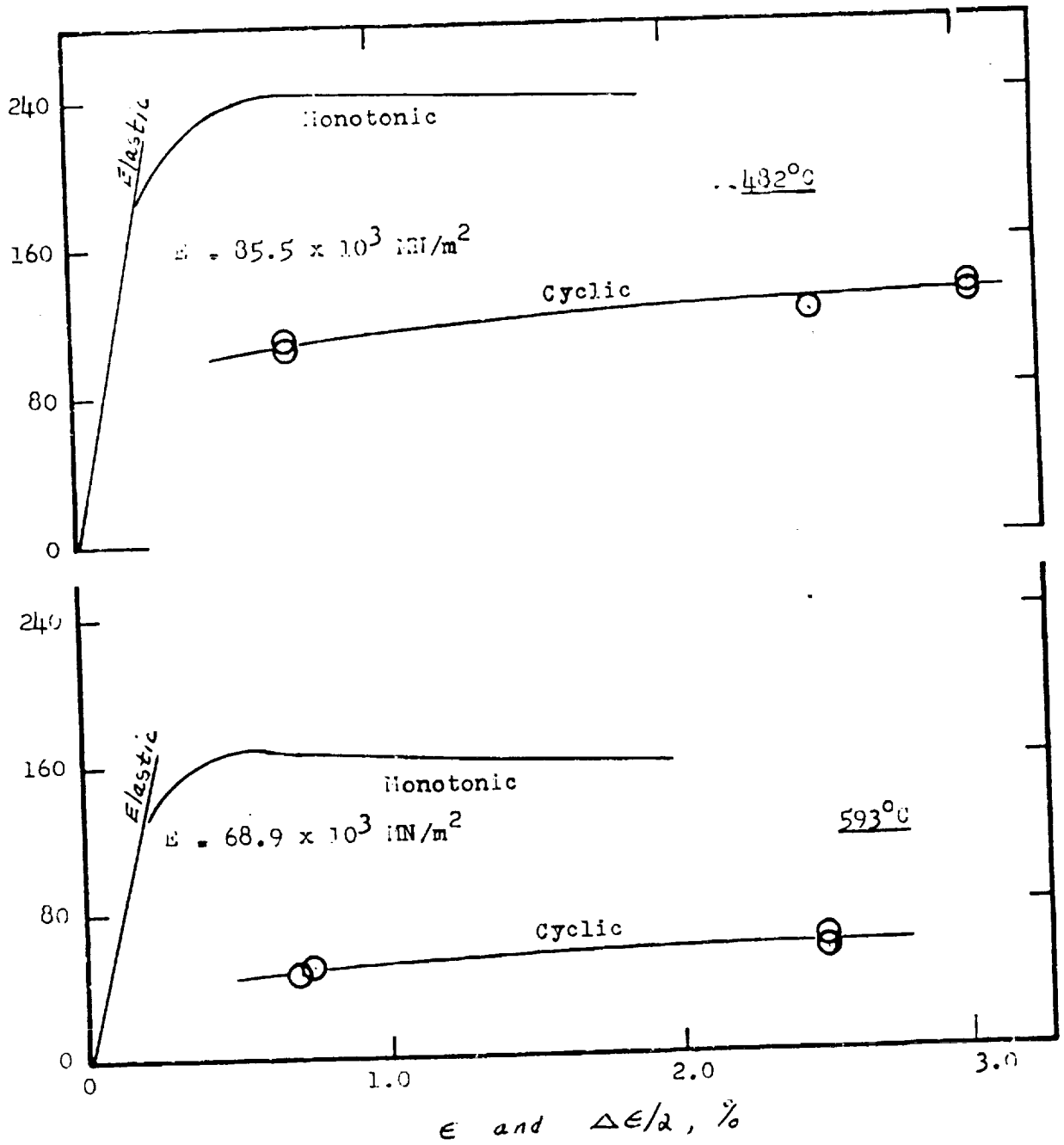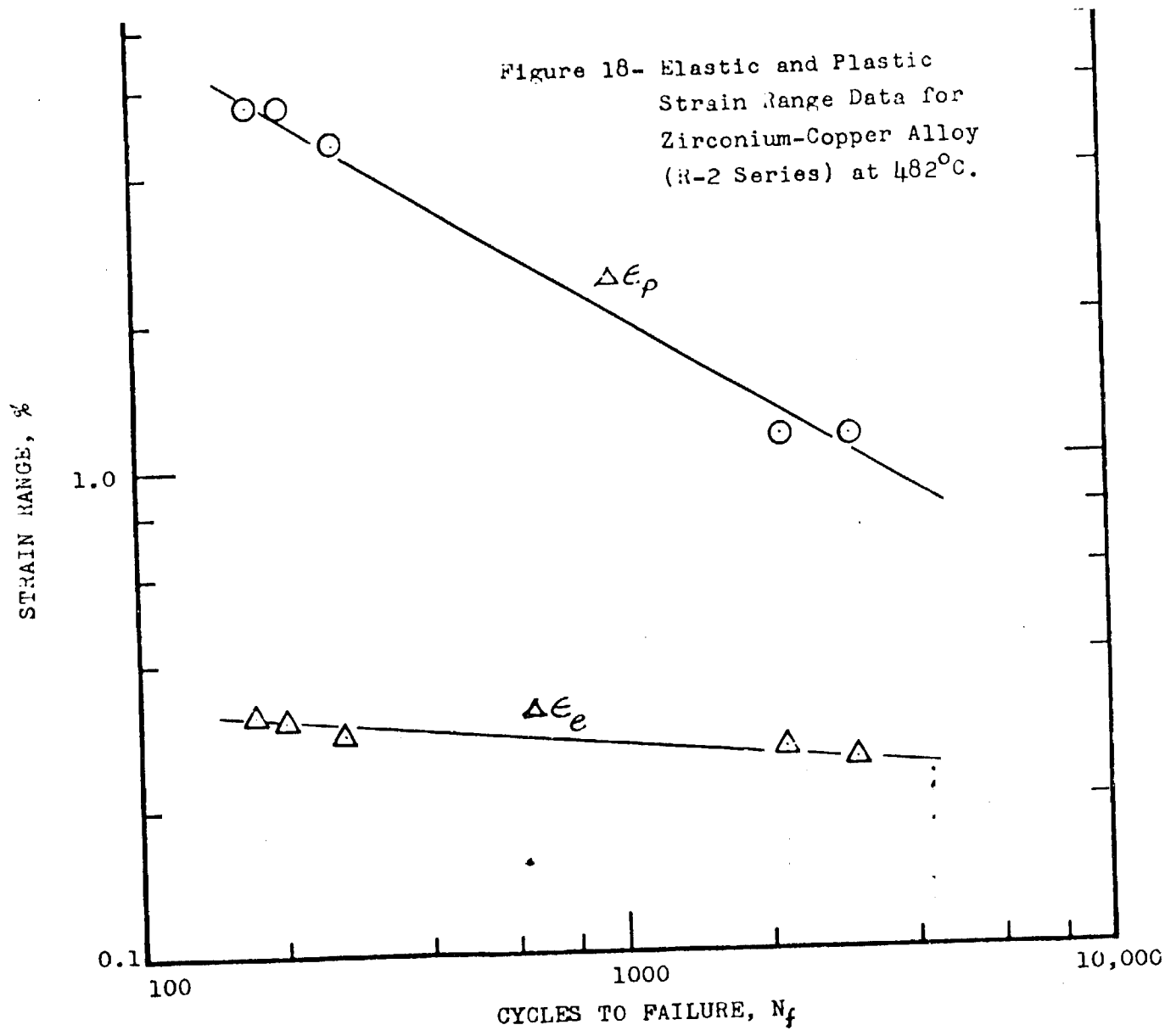
Figure 17 - Monotonic and cyclic stress-strain behavior
of Zirconium-Copper (1/2 hard) alloy measured
in argon at 482°C and 593°C

Figure 18- Elastic and Plastic
        Strain Range Data for
        Zirconium-Copper Alloy
        (R-2 Series) at 482°C.

$\Delta \epsilon_p$

$\Delta \epsilon_e$

STRAIN RANGE, %

1.0

0.1

100

1000

10,000

CYCLES TO FAILURE, $N_f$

42.

in the lower strain range tests (1.4%) at this same strain rate where the test durations were from 30 to 70 hours and in the hold-time tests at the high strain ranges when compression hold periods were involved. And it became particularly severe in the hold-time tests at the lower strain ranges.

An illustration of this behavior is presented in Figure 19 for a few selected R-2 specimens. In Spec. No. R-2-28 (test duration of about 3 hours) the vague beginning of barrelling is indicated by the formation of a zone of metal which is visibly different and which is symmetric above and below the minimum diameter point of the specimen. This zone is easily detected by the fairly distinct boundaries which form as noted in Figure 19. In longer duration tests such as those involving slower strain rates or hold periods, the barrelling becomes more pronounced and the specimen geometry exhibits some drastic changes. Two cases of extreme dimensional instability are shown in Figure 19 for Spec. Nos. R-2-47 and -50. In the one case a "double-necking" region is formed and a slight extension of the specimen length is observed while in Spec. No. R-2-50 a significant increase in diameter on either side of the extensometer location is observed with a decided (about 0.5 cm) shortening of the specimen. Near fracture Spec. No. R-2-50 had the distinct appearance of a notched specimen.

## VII - CONCLUSIONS

This report has presented and discussed the test results obtained during the Task 2 portion of this contract. Following the evaluation of twelve candidate materials on Task 1 of this program, one copper-base alloy having the most potential as a rocket nozzle material was selected for more detailed evaluation during the Task 2 portion of this effort. Short-term tensile, modulus of elasticity, and low-cycle fatigue evaluations were performed to a maximum temperature of 593°C. Special attention was devoted to an assessment of temperature and strain rate effects on short-term tensile and low-cycle fatigue behavior and the effects of hold periods on the low-cycle fatigue life were evaluated at 538°C. In addition, modulus of elasticity measurements were made over the range from room temperature to 593°C. All tensile and fatigue testing was performed in argon using hourglass shaped specimens while the modulus of elasticity measurements were performed in air using cylindrical gage section specimens.

During the Task 2 effort 35 tests were performed in providing the desired information. A detailed summary of the test results is presented in both tabular and graphical form and an analysis of the test data led to the following observations:
   1) the tensile properties were not significantly affected by strain rate at 538°C over the range from $4 \times 10^{-4}$ to $1 \times 10^{-2}$ sec-1;

| R-2-28 | R-2-47 | R-2-50 |
|---|---|---|
| 482°C | 538°C | 538°C |
| 6.1% | 1.4% | 1.4% |
| no hold time | 56 sec(tens.) | 56 sec(comp.) |
| $N_f = 176$ | $N_f = 1,152$ | $N_f = 3,180$ |

Figure 19- Photograph of several tested specimens to illustrate the dimensional instability noted in the R-2 tests.
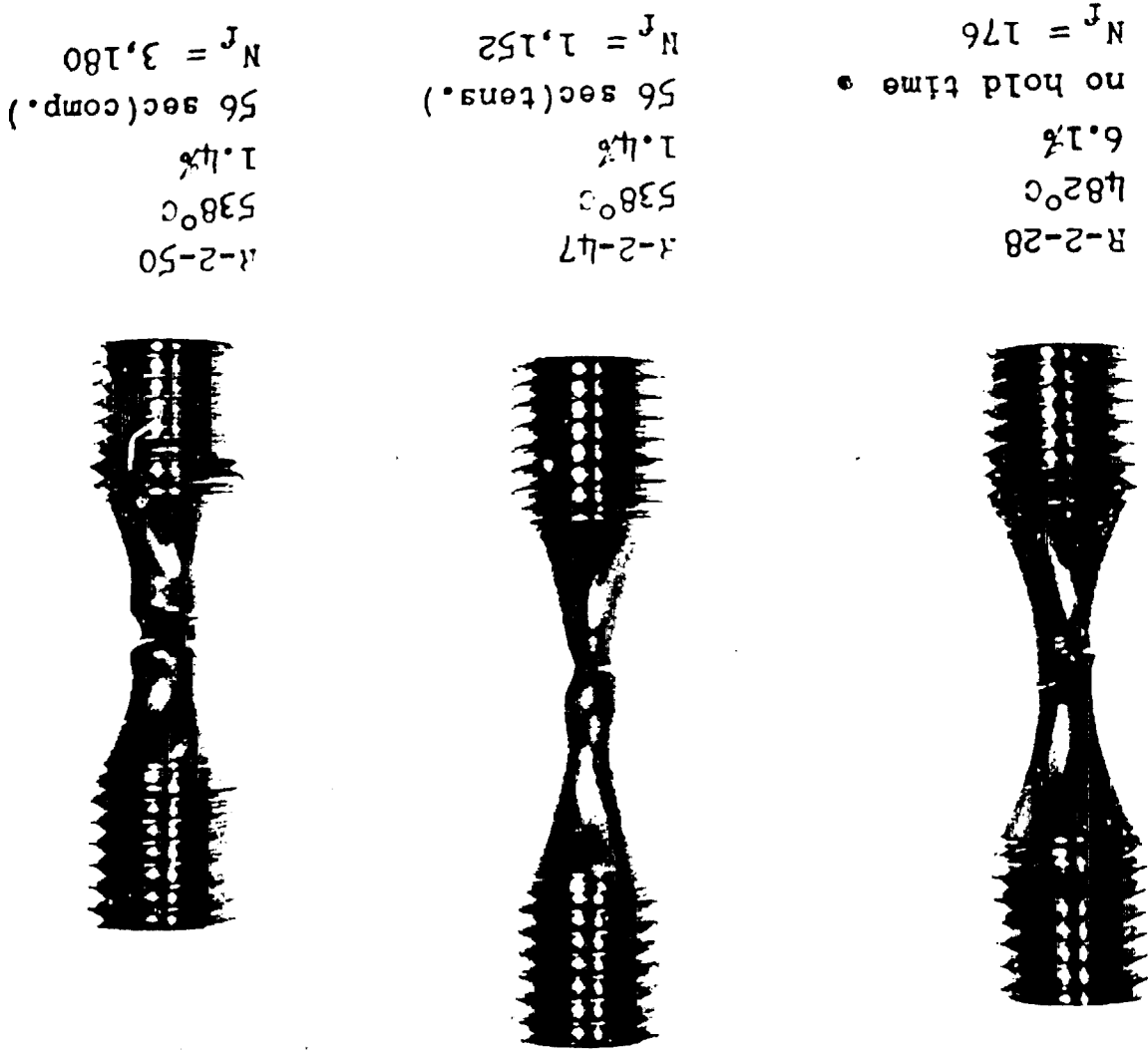
2) the modulus of elasticity decreased from about 115,000 to 70,000 MN/m$^2$ over the temperature span from room temperature to 593°C;

3) the R-2 alloy exhibited a very decided cyclic strain softening;

4) the fatigue life of the R-2 alloy at a strain rate of 2 x 10$^{-3}$ sec$^{-1}$ was unaffected by temperature over the range from 482° to 593°C;

5) the fatigue life of the R-2 alloy at 538°C was decreased as the strain rate decreased;

6) the fatigue life of the R-2 alloy at 538°C was decreased by hold periods in tension; hold periods in compression exerted essentially no effect on the fatigue life;

7) the amount of stress relaxation which occurred during a tension hold period was the same as that observed in a compression hold period of the same duration;

8) after the first fatigue cycle or so the ratio of the stress decrease due to relaxation to the stress level at the start of the hold period remained essentially constant throughout the test.